HHS Public Access

Author manuscript

Curr Biol. Author manuscript; available in PMC 2021 April 20.

Published in final edited form as:

Curr Biol. 2020 April 20; 30(8): 1367–1379.e6. doi:10.1016/j.cub.2020.01.068.

Functions of opsins in *Drosophila* taste

Nicole Y. Leung[1,2], **Dhananjay P. Thakur**[1,2], **Adishthi S. Gurav**[1,2], **Sang Hoon Kim**[3], **Antonella Di Pizio**[4,5,6], **Masha Y. Niv**[4,5], **Craig Montell**[1,2,7]

[1]Neuroscience Research Institute, University of California, Santa Barbara, CA 93106, USA

[2]Department of Molecular, Cellular and Developmental Biology, University of California, Santa Barbara, CA 93106, USA

[3]Department of Biological Chemistry, The Johns Hopkins University School of Medicine, Baltimore, MD 21205, USA

[4]Institute of Biochemistry, Food Science and Nutrition, The Robert H Smith Faculty of Agriculture, Food and Environment, The Hebrew University of Jerusalem, 76100 Rehovot, Israel

[5]The Fritz Haber Center for Molecular Dynamics, The Hebrew University of Jerusalem, 91904 Jerusalem, Israel

[6]Leibniz-Institute for Food Systems Biology at the Technical University of Munich, 85354 Freising, Germany

[7]Lead Contact

Summary

Rhodopsin is a light receptor comprised of an opsin protein and a light-sensitive retinal chromophore. Despite more than a century of scrutiny, there is no evidence that opsins function in chemosensation. Here, we demonstrate that three *Drosophila* opsins, Rh1, Rh4, and Rh7, are required in gustatory receptor neurons to sense a plant-derived bitter compound, aristolochic acid. The gustatory requirements for these opsins are lightindependent and do not require retinal. The opsins enabled flies to detect lower concentrations of aristolochic acid through initiating an amplification cascade that includes a G-protein, phospholipase Cβ, and the TRP channel, TRPA1. In contrast, responses to higher levels of the bitter compound were mediated through direct activation of TRPA1. Our study reveal roles for opsins in chemosensation and raise questions concerning the original roles for these classical G-protein-coupled receptors.

Correspondence: cmontell@ucsb.edu.

Author Contributions

Conceptualization, NYL, SHK, and CM; Methodology, NYL, ADP, MYN, and CM; Validation, NYL; Formal Analysis, NYL; Investigation, NYL, DT, ASG, ADP, and MYN; Writing – Original Draft, NYL and CM; Writing – Review & Editing, NYL, ADP, MYN and CM; Visualization, NYL and CM; Supervision, CM; Project Administration, CM; Funding acquisition, CM.

Declaration of Interests

The authors declare no competing interests.

DATA AND CODE AVAILABILITY

This study did not generate/analyze datasets or code.

Graphical Abstract

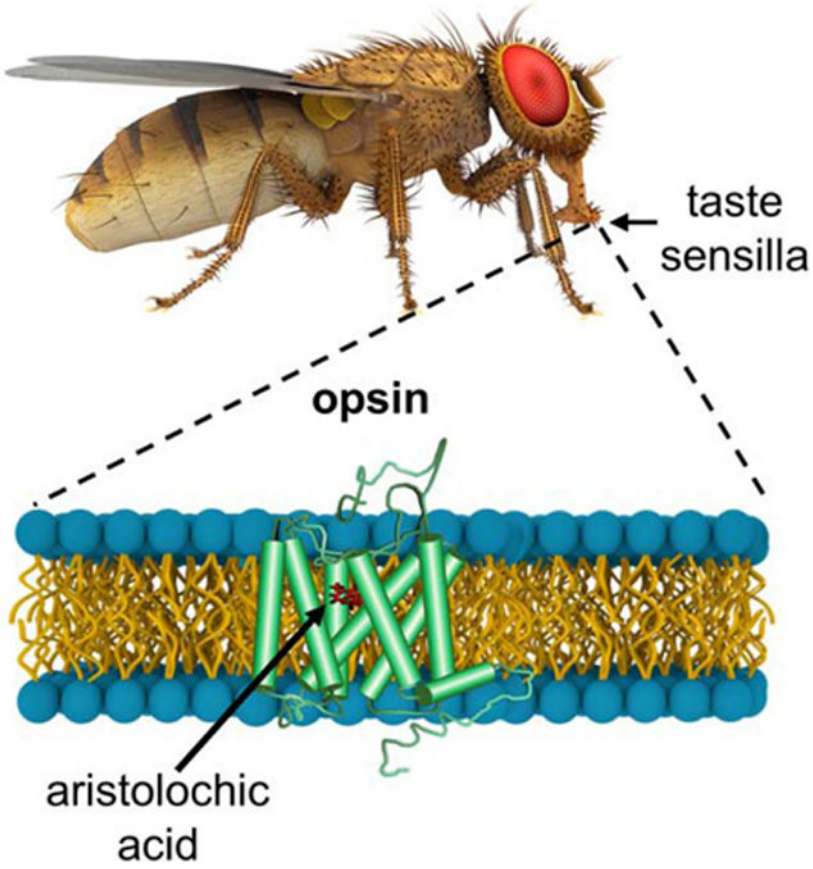

Keywords

Drosophila; opsin; rhodopsin; gustatory; GPCR; phospholipase C; labellum; TRP channel; retinal; chromophore

Introduction

Animals rely heavily on contact chemosensation to evaluate food quality, such as flavor and nutritional value. The chemical perception of food is initiated through the binding of tastants to receptor proteins that are expressed in specialized peripheral gustatory receptor cells [reviewed in 1]. The information is then delivered to the central nervous system, ultimately contributing to the decision to ingest or reject the food. Thus, peripheral taste coding is essential for an animal to avoid consuming harmful substances, which are often bitter.

To date, all taste receptors identified in insects are known or putative ion channels [reviewed in 1]. The employment of ligand-gated cation channels in sensing attractive and aversive compounds in insects differs greatly from mammalian sweet, bitter, and umami tastes, which function through signaling cascades that are initiated by G-protein-coupled receptors (GPCRs). Once activated, mammalian taste receptors subsequently couple to a

phospholipase C (PLC)-dependent signaling cascade, which culminates with activation of the Transient Receptor Potential (TRP) channels, TRPM4 and TRPM5 [2–5]. A limitation of ionotropic receptors that are used in fly taste is that they do not allow for signal amplification, which would enable detection of chemicals at lower levels than would otherwise be possible. A hint that a mammalian-like taste transduction cascade exists in insects is the finding that gustatory detection of the plant-derived bitter compound, aristolochic acid, depends on a PLCβ and TRPA1 [6].

In this study, we found that three *Drosophila* opsins, Rh1, Rh4, and Rh7, are required for sensation of aristolochic acid but only at lower concentrations. While lower levels of aristolochic acid are detected through an opsin-initiated signaling cascade coupled to G_q, PLCβ, and TRPA1, flies respond to higher concentrations of the same chemical through direct activation of TRPA1. These findings provide the first demonstration that opsins function in chemosensation since their discovery in the 19th century [7–9, reviewed in 10]. Given the recent findings that rhodopsins contribute to thermosensation, hearing, and proprioception [11–14], we propose that rhodopsins represent a class of polymodal sensory receptor with roles potentially as diverse as TRP channels.

Results

Requirements of Rh1, Rh4, and Rh7 for avoiding aristolochic acid

The requirement for PLCβ and TRPA1 for sensing aristolochic acid [6] raised the possibility that one or more GPCRs are the receptors that initiate the signaling cascade coupled to these proteins. We tested whether opsins are the GPCRs since their activities are linked to PLCβ. We allowed flies to choose between 2 mM sucrose alone versus 2 mM sucrose plus aristolochic acid, mixed with red or blue food dye. We inspected the color of the abdomens and calculated a preference index (PI). A PI = 1.0 or −1.0 results from complete preference for one or the other food, while a PI = 0 indicates indifference to the two options. The red food coloring at 0.2 mg/mL or blue coloring at 0.08 mg/mL did not cause bias when combined with sucrose only (Figure S1A). Moreover, the flies displayed similar repulsion to 1 mM aristolochic acid regardless of the dye color (Figure S1B; PI = 0.58 ±0.03 and 0.52 ±0.03). The aversion to aristolochic acid displayed the steepest dose-dependence at concentrations ≤1.0 mM (Figure 1A).

We screened all seven *opsin* mutants for defects in avoiding 1 mM aristolochic acid. While mutations disrupting four of the opsins had no impact relative to control flies, we found significant impairments in avoidance due to null mutations affecting any of three *opsin* genes: *rh1* (also known as *ninaE*), *rh4*, and *rh7* (Figure 1B; PI = 0.34 ±0.03, 0.33 ±0.02, and 0.39 ±0.02, respectively). In contrast, the GR66a and GR33a gustatory receptors, which function in the taste avoidance of many aversive compounds [15–18], were dispensable for sensing aristolochic acid (Figure S1C).

Each of the three *opsin* mutations also displayed defects in avoiding aristolochic acid when placed *in trans* with deficiencies that removed the corresponding genes ($rh1^{I17}$/Df, $rh4^{1}$/Df, and $rh7^{1}$/Df) (Figure S1D). The distaste for 1 mM aristolochic acid exhibited by the double mutants ($rh4^{1}$,$rh1^{I17}$, $rh7^{1}$,$rh1^{I17}$, and $rh7^{1}$,$rh4^{1}$) and triple mutants

($rh7^1$,$rh4^1$,$rh1^{I17}$) were greatly reduced compared to the control (Figure 1B; PI = 0.20 ±0.04, 0.18 ±0.04, 0.23 ±0.02, and 0.12 ±0.02, respectively). The differences between single and double mutants, and single and triple mutants were mostly significant, although the slightly lower preference index exhibited by the triple mutant relative to the double mutants was not significant (Table S1).

Opsins function in bitter-responsive GRNs for sensing aristolochic acid

We performed extracellular electrophysiological recordings (tip recordings) to examine whether Rh1, Rh4, and Rh7 function in gustatory receptor neurons (GRNs). Each bilaterally symmetrical labellum contains ~31 bristles (sensilla), each of which houses two or four GRNs [reviewed in 1]. Taste sensilla are categorized into three classes, including small (S-type) sensilla, most of which respond to aversive tastants. We recorded from S6 sensilla because they contain GRNs that display the highest frequencies of aristolochic acid-induced action potentials [6, 19]. Upon stimulation with 1 mM aristolochic acid, control flies exhibited 19.8 ±2.7 spikes/sec (Figures 1C and 1D). We found that flies lacking Rh1, Rh4, or Rh7 showed large decreases in neuronal firing (Figures 1C and 1D; 5.8 ±1.4, 7.8 ±2.4, and 6.1 ±2.0 spikes/sec, respectively). We observed similar reductions in action potentials when we placed each mutation *in trans* with the corresponding deficiencies (Figures S1E and S1G). The single, double, and triple mutants exhibited similar decreases in action potential firing in response to 1 mM aristolochic acid (Figures 1C, 1D, and S1H). This differs from the significantly greater deficits in behavior between the single and double mutants (Table S1). However, it is difficult to precisely correlate concentrations of tastants used for behavior and tip recordings since the latter involves placing chemicals in a recording electrode, which directly contacts the endolymph surrounding the dendrites. Therefore, we performed tip recordings using slightly lower levels of aristolochic acid (0.5 mM) and found that the triple mutant (TM) produced fewer action potentials than the single mutants (Figure S1F). Nevertheless, because the action potential frequencies were already low with the single mutants, the further reduction in the triple mutant was not statistically significant.

Only one bitter-responsive GRN is housed in a sensillum, suggesting that the opsins function in the same GRNs. To address this possibility, we first determined whether all of the opsins function in bitter-responsive GRNs. We tested whether we could rescue the $rh1^{I17}$, $rh4^1$, and $rh7^1$ mutant phenotypes using the corresponding rescue transgenes driven by *Gr66a-GAL4*, which directs expression in bitter-responsive GRNs [20]. We found that the behavioral (Figures 2A–2C) and electrophysiological impairments (Figures 2D–2F and S2A–S2C) in responding to aristolochic acid were all rescued indicating that the opsins function in bitter-responsive GRNs. To test whether the opsins function in the same GRNs, we used the *rh1-GAL4* and *rh4-GAL4* to drive expression of the various *UAS-opsin* transgenes, in each of the three mutant backgrounds. The *rh1GAL4* and *rh4-GAL4* were both effective for this purpose since they rescued the mutant phenotypes exhibited by the $rh1^{I17}$ and $rh4^1$ mutants when we combined them with *UAS-rh1* and *UAS-rh4*, respectively (Figures S2D–S2F). The *rh1-GAL4* and *rh4-GAL4* also rescued each of the mutant phenotypes when we used them to drive the corresponding rescue transgenes (Figures 2A–2F and S2A–S2C), indicating that the opsins function in the same GRNs.

Gustatory roles of opsins do not require the chromophore

Rh1, Rh4, and Rh7 are light sensors [21, 22], raising the question as to whether aristolochic acid repulsion is affected by light. The two-way choice feeding assays were performed in the dark, suggesting that the behavior is not light dependent. To test whether light affects aristolochic acid repulsion, we compared the behavior in the dark and light, and found that avoidance was not significantly different (Figure 3A). Moreover, bright light did not significantly affect aristolochic acid avoidance in flies expressing *opsin* transgenes under control of the *Gr66a-GAL4* driver (Figure S3A).

In fly photoreceptor cells, the chromophore (3-hydroxy-11-*cis*-retinal) serves as a light sensor and as a molecular chaperone, which is required for the rhodopsin to exit the endoplasmic reticulum [23, 24]. Therefore, even though the roles for the opsins in sensing aristolochic acid were light-independent, we could not exclude that the retinal is required for chemosensation. To test this question, we eliminated a scavenger receptor, NINAD, which promotes the uptake of carotenoids in the midgut [25–27]. However, the $ninaD^{1}$ mutant flies still produced a substantial light response, as assessed by performing electroretinogram recordings (Figures 3B and 3C). We reduced chromophore levels further by maintaining $ninaD^{1}$ flies on carotenoid-free food, and did so for multiple generations to minimize maternal transfer of retinoids. Although there was virtually no light response after one or two generations on this diet (Figures S3B and S3C), we continued to maintain $ninaD^{1}$ flies on carotenoid-free food for three generations ($ninaD^{1}$ F3). We found that the $ninaD^{1}$ F3 flies, which were unresponsive to light (Figure 3D), showed normal aversion to 1 mM aristolochic acid (Figure 3E) and a normal frequency of aristolochic acid-induced action potentials compared to controls maintained on standard food (Figures 3F and 3G). These results indicate that the chromophore is dispensable for taste.

We further tested whether the retinal is dispensable for sensing aristolochic acid by introducing an amino acid substitution in Rh1 that prevents it from binding the chromophore. Retinal forms a covalent linkage with a lysine in the seventh transmembrane domain of opsins [28] (residue 319 in Rh1) [29, 30]. Therefore, we changed lysine 319 to an arginine, and expressed the $UAS\text{-}rh1^{K319R}$ transgene in a $rh1^{I17}$ null background using the *Gr66a-GAL4*. We found that $rh1^{K319R}$ flies showed normal aristolochic acid repulsion (Figure 3H) and normal aristolochic acid-induced action potentials (Figures 3I and 3J). Together, these data demonstrate that the Rh1 apoprotein is sufficient for functioning in the gustatory response.

Requirement for opsins in adults for gustatory avoidance of aristolochic acid

Rhodopsins are expressed at extremely high levels in photoreceptor cells for efficient photon capture. However, the contributions of *rh1*, *rh4*, and *rh7* to taste are not affected by light suggesting that they may be expressed at low levels in GRNs, potentially to avoid photon capture. Indeed, we were unable to detect opsin proteins in GRNs using Rh1, Rh4, or Rh7 antibodies, even after tyramide amplification. Therefore, we employed RT-PCR as well as quantitative RT-PCR (RT-qPCR) to assay for *opsin* RNA expression in the labellum. Using these approaches, we detected *rh1*, *rh4*, and *rh7* transcripts in the labellum of control flies (RT-PCR, Figures 4A–4C; RT-qPCR, Figures 4D–4I). The signals were specific as they were

absent in the null mutants (Figures 4A–4I). As described above, light did not interfere with aristolochic acid avoidance even when we expressed the opsins in bitter GRNs using the *Gr66a-GAL4* driver (Figure S3A). However, GRNs do not include microvilli, which in fly photoreceptor cells enable rhodopsins to accumulate to high levels necessary for efficient photon capture. Thus, the lack of light sensitivity may be due to the combination of low expression of the opsins and minimal retinal in the GRNs.

The question arises as to whether the opsins function in bitter taste in the adult, or whether the defects in aristolochic acid sensation in the opsin mutants reflect roles during development. Therefore, we conducted tissue-specific, temperature-controlled RNAi-mediated knockdown of *rh1*, *rh4*, and *rh7* using the *Gr66a-GAL4* driver, which is expressed ubiquitously in bitter GRNs. To temporally control the activity of the GAL4 transcription factor, we employed a transgene encoding a temperature-sensitive GAL4 repressor ($GAL80^{ts}$), which is expressed under the control of the *tubulin* promoter (*tubulin-GAL80^{ts}*). $GAL80^{ts}$ is functional at 18°C and inhibits GAL4 activity, thereby preventing RNAi-mediated knockdown at 18°C. At 29°C, the $GAL80^{ts}$ is inactive. Consequently, RNAi knockdown occurs at 29°C. To ind uce RNAi knockdown only in the adults, we raised flies at 18°C and then shifted the animals to 29°C upon eclosion. We then performed two-way choice feeding assays and tip recordings on 5-day old flies.

We found that knockdown of *rh1*, *rh4*, and *rh7* in the adult stage resulted in defects in the gustatory sensation of aristolochic acid. These include impairments in behavioral avoidance of aristolochic acid and reductions in action potentials (18°→29°; Figures 4J and 4K). This was not due to effects of temperature alone since there were no differences in aristolochic acid-induced avoidance or action potentials at 18° and 29°C in the absence of an RNAi transgene (Figures 4J and 4K). Moreover, when we maintained the flies at 18°C during development and in adults, there were no reductions in aristolochic acid responses (18°→18°; Figures 4J and 4K). These data demonstrate that the opsins are required in the adult for the gustatory responses to aristolochic acid, and the mutants do not cause deficits in aristolochic acid taste due to a role for opsins during development.

To provide an additional test of the finding that the *opsin* mutations do not cause a developmental defect in GRNs, we examined responses to other bitter compounds that are detected by the same GRNs as aristolochic acid. We found that the S6 sensilla from the *opsin* triple mutant (*rh7^{1}*,*rh4^{1}*,*rh1^{I17}*) showed a similar number of action potentials to denatonium, strychnine, and quinine as control flies (Figures S4A–S4C). Since there is only one bitter-responsive GRN in these sensilla, these results demonstrate that this GRN was still functional in the triple mutant, and specifically lacked a response to aristolochic acid. Consistent with these results, the avoidances to denatonium, strychnine, and quinine were indistinguishable between control and *rh7^{1}*,*rh4^{1}*,*rh1^{I17}* flies (Figures S4E–S4G). The triple mutant also exhibited normal gustatory responses to sucrose (Figures S4D and S4H). Further indicating that the deficit in aristolochic acid taste is not due to a developmental defect, the morphology of *Gr66a*-positive GRNs, including the bitter-responsive GRN in S6 sensilla, were indistinguishable between the *opsin* mutants and the control (Figures S4I–S4L).

Since we used the *opsin-GAL4*s to rescue the various opsin phenotypes, yet the drivers were not sufficiently strong to reveal reporter staining, the question arises as to whether the *GAL4*s are capable of driving expression in the labellum. To address this issue, we focused on the *rh1-GAL4* and conducted RT-qPCR experiments using the *rh1-GAL4* and *UAS-rh1* in a null $rh1^{I17}$ background. We observed increases in *rh1* transcript levels in the labella of *rh1-GAL4>UAS-rh1*;$rh1^{I17}$ flies relative to flies harboring the *UAS-rh1* transgene only in a $rh1^{I17}$ background (Figure S4M). These data indicate that the *rh1-GAL4* directs expression in the labellum, thereby providing an explanation as to how the driver can rescue the phenotype. The presence of low levels of *rh1* transcripts in control flies (*UAS-rh1*;$rh1^{I17}$) is presumably due to residual genomic DNA in the RNA preparation, following DNAse I treatment.

Activation of Rh7 by bitter compounds *in vitro*

To test whether the opsins are chemical receptors, we set out to express them in tissue culture cells to determine whether they are activated by aristolochic acid. Functional expression of most *Drosophila* opsins in heterologous systems has not been successful due to their inability to exit the endoplasmic reticulum. Indeed, Rh1 and Rh4 remain in the endoplasmic reticulum when expressed in HEK293T cells (Figures S5A and S5B). However, we can effectively express Rh7 and detect an extracellular Nterminal FLAG tag (Figure 5A) [22]. We did not detect either Rh1 or Rh4 on the cell surface even after substituting the N- and C-terminal regions of these opsins with the corresponding versions of Rh7 (Figures S5A and S5B). Moreover, Rh7 was also retained in the endoplasmic reticulum of HEK293T cells when co-expressed with Rh1 or Rh4. Therefore, we focused the following analysis on Rh7.

To determine whether Rh7 can be activated by aristolochic acid, we used an approach that takes advantage of β-arrestin binding to an activated GPCR [31]. In this assay, β-arrestin is fused to a TEV protease, while the GPCR is linked to a tTA transcriptional activator with an intervening TEV protease cleavage site (TEVpcs). Upon recruitment of the β-arrestin-TEV protease fusion protein to the activated GPCRTEVpcs-tTA chimera, the tTA is released from the GPCR, leading to expression of a luciferase reporter.

We found that Rh7 was activated by aristolochic acid in a dose-dependent manner (EC_{50} = 0.28 pM; Figure 5B). Piperonyl acetate is structurally similar to aristolochic acid (Figure 5D) and is a bitter compound [32]. Rh7 was also activated by piperonyl acetate (EC_{50} = 2.29 nM; Figure 5C). Consistent with these data, 1 mM piperonyl acetate is repulsive to control flies, and this aversion is significantly reduced in *opsin* mutant flies (Figures 5E).

We also tested whether ectopic expression of any of the opsins *in vivo* confers responsiveness to aristolochic acid. Sugar-responsive GRNs express PLC [33, 34]. Therefore, we expressed *UAS-rh1*, *UAS-rh4*, or *UAS-rh7* under control of the *Gr5aGAL4* driver, which is expressed in sugar-responsive GRNs [35]. We found that expression of *rh7*, but not *rh1* or *rh4*, generated aristolochic acid-induced action potentials (Figures 5G and 5H). Moreover, the response by sugar-responsive GRNs expressing *rh7* required a high concentration of aristolochic acid (5 mM), and the frequency of action potentials was relatively low (Figure 5H; 3.5 ±0.9 spikes/sec). The low frequency of action potentials was not due to impairments in the sugar GRNs since the flies exhibited normal sucrose responses

(Figure 5I). The results that only Rh7-expressing sugar GRNs display aristolochic acid-induced action potentials is consistent with our findings that in HEK293 cells, Rh7 is functionally expressed but Rh1 and Rh4 are retained in the endoplasmic reticulum. Furthermore, the low sensitivity of Rh7expressing sugar-responsive GRNs to aristolochic acid supports the mutant analyses in bitter GRNs, suggesting that all three opsins are required in the same cells for high sensitivity to this chemical.

Modeling of bitter compound binding to Rh7

We performed homology modeling of Rh7 using the crystal structures of human, bovine, and squid rhodopsins as templates (GPCR-I-TASSER; [36]. Using induced-fit docking simulations, we investigated the aristolochic acid and piperonyl acetate binding to the GPCR orthosteric ligand pocket and found that both chemicals fit into a similar binding pocket as retinal (Figure S5C and S5D). Aristolochic acid appeared to establish polar interactions with K374, and hydrophobic interactions with F286 and Y346 (Figure S5C). Most of the residues in Rh7 that are predicted to interact with aristolochic acid are conserved in Rh1 and Rh4 (Table S2). Piperonyl acetate appears to interact with the same residues, including a hydrogen bond with K374, and aromatic interactions with F286 and Y346 (Figure S5D).

Opsins couple to a signaling cascade to sense lower concentrations of aristolochic acid

In photoreceptor cells, rhodopsin-dependent signaling amplifies responses to dim light. Therefore, we wondered if Rh1, Rh4, and Rh7 were specifically required for sensing lower levels of aristolochic acid. We compared the behavior of the *opsin* triple mutant flies using 1 mM and 5 mM aristolochic acid. In contrast to the strong impairment in response to 1 mM aristolochic acid, $rh7^{1}$,$rh4^{1}$,$rh1^{I17}$ flies did not show a significant deficit in avoiding 5 mM aristolochic acid (Figures 6A and 6B; PI = 0.20 ±0.02 and 0.69 ±0.02, respectively). These results were mirrored by concentration-dependent effects on neuronal firing of GRNs. Elimination of the opsins caused a dramatic attenuation in action potentials in response to 1 mM aristolochic acid (Figures 6C and S6A; 6.6 ±1.4 spikes/sec), while the triple mutant displayed normal neuronal activity upon exposure to 5 mM aristolochic acid (Figures 6D and S6B; 23.6 ±2.3 spikes/sec). The *opsin* mutants also responded normally to the higher concentration of piperonyl acetate (5 mM; Figure 5F).

The rhodopsins in fly photoreceptor cells initiate a signaling cascade that engages a trimeric G-protein (G_q), a PLCβ (NORPA), and culminates with activation of the TRP and TRPL channels [37–41]. Therefore, the opsins might couple to a similar pathway in GRNs. If so, $G_{\alpha q}$ and NORPA might function in GRNs for sensing lower (1 mM) but not higher (5 mM) concentrations of aristolochic acid. We assayed behavioral responses and neuronal firing in $G_{\alpha q}^{1}$ and $norpA^{36}$ mutant flies, along with each mutant over the corresponding deficiency, and found large reductions in avoidance and action potentials to 1 mM aristolochic acid (Figures 6A, 6C, and S6A). However, these flies responded normally to 5 mM aristolochic acid, with the exception of $G_{\alpha q}^{1}$ mutant flies, which exhibited a slight defect in the behavioral response only (Figures 6B, 6D, and S6B).

Mutation of *trpA1-CD* disrupts aristolochic acid taste

We previously showed that the gustatory avoidance of aristolochic acid depends on TRPA1 [6]. Our data suggest that lower levels of aristolochic acid (1 mM) primarily activate TRPA1 indirectly since the responses to this concentration depend on opsins, $G_{\alpha q}$, and NORPA. However, TRPA1 may be effectively activated directly by 5 mM aristolochic acid since the detection of this concentration is independent of the opsins, $G_{\alpha q}$ and NORPA. Therefore, we tested whether the $trpA1^{1}$ null mutant displays impairments in the responses to 1 mM and 5 mM aristolochic acid. We found that at both of these concentrations, aristolochic acid-induced action potentials were nearly eliminated (Figures 7A, 7B and 7M). While the electrophysiological responses to aristolochic acid are virtually eliminated in the $trpA1^{1}$ mutant, there is a remaining aversion to aristolochic acid (Figure 7C and 7D). The behavioral avoidance in the $trpA1^{1}$ mutant is most likely due to the observations that in addition to activating bitterresponsive GRNs, which induces aversion, bitter compounds also suppress sugarresponsive GRNs, thereby decreasing attraction to sugars [42–44].

We combined each *opsin* mutation with $trpA1^{1}$, and found that in response to 1 mM aristolochic acid, the double mutants showed comparable electrophysiological phenotypes to $trpA1^{1}$ alone, consistent with the conclusion that they function in a common pathway (Figure S7A). Because the opsins are dispensable for responding to 5 mM aristolochic acid, the double mutants also showed similar deficits in the electrophysiological responses as the $trpA1^{1}$ mutant alone (Figure S7B). Further evidence consistent with the model that the opsins and TRPA1 function in a common pathway, the chemical specificity of TRPA1 was reminiscent of the opsins, as TRPA1 was not required for the responses to denatonium, strychnine, denatonium (Figures S4A–C and S4E–G), or sucrose (Figures S4D and S4H).

The *trpA1* gene encodes several isoforms [45]. The A and B isoforms (AB) share a common promoter [45–48], while the C and D isoforms (CD) share a different promoter [45, 47, 48] (Figure S7C). We found that removal of the AB isoforms ($trpA1\text{-}AB^{GAL4}$) had no impact on the avoidance or electrophysiological responses to 1 mM or 5 mM aristolochic acid (Figures 7A–7D and 7M). In contrast, deletion of the CD isoforms ($trpA1\text{-}CD^{GAL4}$) significantly impaired repulsion and reduced neuronal firing to 1 mM and 5 mM aristolochic acid, similar to the $trpA1^{1}$ mutant (Figures 7A–7D and 7M).

Expression patterns of *trpA1* isoforms

To address whether the *trpA1-CD* isoforms are expressed in GRNs in the labellum, we used the *GAL4* knock-in ($trpA1\text{-}CD^{GAL4}$) to drive expression of *UAS-dsRed*. We found that the CD^{GAL4} reporter was broadly expressed in GRNs (Figure 7E). A subset of these GRNs overlapped with a marker that labels bitter-responsive GRNs (*Gr66a-I-GFP*; Figures 7F and 7G), but not with a marker that labeled sugar-responsive GRNs (*Gr5a-I-GFP*; Figures 7H–7J and S7J). The *GAL4* reporter for the *trpA1-AB* isoforms ($trpA1\text{-}AB^{GAL4}$) drove expression of *UAS-dsRed* in a subset of bitter-responsive GRNs, but not the sugar-responsive GRNs (Figures S7D–S7I and S7K).

We examined the distribution of the AB^{GAL4} and CD^{GAL4} reporters in the brain and legs using the *UAS-mCD8::GFP* reporter. In the brain, the AB^{GAL4} labeled the fan-shaped body

(FB) and the gustatory center—the subesophageal zone (SEZ; Figure S7M), and the *CD*^{GAL4} stained the SEZ and antennal lobes (AL; Figure S7O). We also examined expression of the *AB*^{GAL4} and *CD*^{GAL4} reporters in the tarsal segments of the pro-thoracic legs. The cuticle of the tarsi produces autofluorescence with *UAS-GFP* only, but there is no autofluorescence corresponding to cells (Figure S7L). The *AB*^{GAL4} fluorescent was indistinguishable from the *UAS-GPF* only control (Figures S7N and S7N‘), while the *CD*^{GAL4} stained neuronal processes and cell bodies in multiple segments (Figure S7P).

Activation of TRPA1-D by aristolochic acid

The preceding data suggest that either the TRPA1-C or TRPA1-D isoform may be directly activated by aristolochic acid, and more robustly at the higher (5 mM) than lower levels (1 mM). We expressed these proteins in *Xenopus* oocytes and performed two-electrode voltage clamp recordings. Unlike many TRPA1 isoforms that are strongly activated by allyl isothiocyanate (AITC) [49–51], TRPA1-C is very mildly responsive to AITC and showed no activity upon addition of aristolochic acid, even at a concentration of 5 mM (Figure 7K). However, TRPA1-D, which was robustly stimulated by AITC, showed dose-dependent activation by aristolochic acid starting at 0.5 mM and was strongly responsive at 5 mM (Figure 7L). Moreover, we restored normal behavioral and electrophysiological responses to 1 mM and 5 mM aristolochic acid in *trpA1-CD*^{GAL4} mutant flies by expressing the *UAS-trpA1-D* transgene under control of the *GAL4* knocked into the *trpA1-CD*^{GAL4} allele (Figures 7A–7D; labeled *D*;*CD*). Unexpectedly, we observed partial rescue using the *trpA1-C* transgene (Figures 7A—7D; labeled *C*;*CD*). Therefore, while we cannot exclude a role for the C isoform, but conclude that TRPA1-D is directly activated by aristolochic acid.

Discussion

Opsin apoprotein functions independent of retinal in taste

In this study, we demonstrate that opsins function in *Drosophila* taste. In support of this conclusion, mutation of *rh1*, *rh4*, or *rh7* reduced the behavioral and electrophysiological responses to lower levels of aristolochic acid. The opsins function in GRNs since we fully rescued the mutant phenotypes by introducing wild-type transgenes specifically in bitter-responsive GRNs. While we detected opsin transcripts in the labellum, opsin expression was below the levels detectable with antibodies or with the *opsin* reporters. We propose that the low expression of opsins in GRNs provides a mechanism to prevent light from interfering with gustatory responses. Consistent with this proposal, the functions of opsins in GRNs are light independent.

In photoreceptor cells, opsins bind to retinal, which is the light-sensitive component of rhodopsin. In fly eyes, retinal is also required for rhodopsins to exit the endoplasmic reticulum [24]. In thermosensory, auditory, and proprioceptive neurons that depend on rhodopsins for temperature discrimination, hearing, and locomotion, the retinal is also essential, even though the roles of rhodopsins in these neurons are light independent [11–14]. Presumably, this reflects the chaperone function of the retinal. However, the chromophore is not required for the function of opsins in chordotonal neurons [52].

We found that retinal is dispensable in GRNs for opsin function since *ninaD*^{1} mutants raised on carotenoid-free food respond normally to aristolochic acid. Moreover, mutation of the lysine critical for binding retinal does not prevent detection of aristolochic acid by Rh1. Therefore, retinal does not serve as a molecular chaperone for opsins in GRNs. An open question concerns the molecular and cellular explanation as to how opsins can bypass a chaperone requirement for retinal in some neurons, such as GRNs and chordotonal neurons.

Opsins are chemosensors

An important issue is whether or not opsins function directly as chemosensors. This is challenging to address since *in vitro* expression of most insect opsins is problematic because they are not trafficked to the plasma membrane. Rh7 is an exception, as it can be functionally expressed in HEK293T cells [22]. We demonstrate that aristolochic acid, and a structurally similar chemical, piperonyl acetate, stimulate dose-dependent increases in Rh7 activity. Based on these findings, we propose that Rh7 is activated directly by aristolochic acid and piperonyl acetate. Our structural modeling suggest that these ligands occupy a similar binding site as retinal. The observation that retinal is dispensable for sensing these tastants supports this model, as the retinal binding site is available for binding other ligands. Rh7 might be part of a heteromultimeric receptor that include Rh1 and Rh4, and the sensitivity for aristolochic acid and piperonyl acetate might be increased by a heteromultimeric opsin receptor. However, it was not possible to functionally express Rh1 or Rh4 in HEK293T cells since they are retained in the endoplasmic reticulum.

Functioning of multiple opsins in the same bitter-responsive GRNs

Rh1, Rh4, and Rh7 appear to function in the same GRNs since we rescued the phenotype of each mutant by driving expression of the corresponding wild-type transgene with the transcriptional control region of a different *opsin* gene. Co-function of multiple opsins in the same GRNs differs from most photoreceptor cells [21]. However, Rh3 and Rh4 act together in a subset of photoreceptor cells near the dorsal rim of the *Drosophila* eye [53], and rhodopsins are co-expressed in R7 cells of mosquitoes [54] Moreover, two or more opsins function in the same thermosensory, auditory, and proprioceptive neurons in flies [11–14]. Two visual pigments (S and M opsins) are also co-expressed in a subset of mouse cone cells [55].

Until recently, GPCRs were generally thought to be comprised of homo- or heterodimers [reviewed in 56, 57, 58]. However, a series of recent studies indicate that at least some GPCRs function as tetramers through association of two homo- and/or heterodimers [59–65]. Thus, three opsins may form a heteromultimer in GRNs. The concept that bitter taste receptors consist of more than two subunits may also extend to the mammalian bitter receptors, T2Rs, which are GPCRs. Multiple T2Rs respond to the same bitter compound and appear to be co-expressed in the same taste receptor cells [66–69].

Evolutionary conservation of GPCR signaling in taste

Many mammals, such as mice and humans, sense bitter, sweet, and umami tastes through a GPCR/G_q/PLC/TRP signaling cascade [reviewed in 1]. This differs from gustatory sensation in flies, which is accomplished primarily through activation of ionotropic receptors, such as

"gustatory receptors" (GRs). Our findings that Rh1, Rh4, and Rh7 operate in sensing aristolochic acid through a cascade that also includes a G_q, PLC, and a TRP channel demonstrate that the repertoire of gustatory strategies used by flies includes a signaling cascade reminiscent of mammalian taste transduction. Thus, GPCR signaling in taste is evolutionary conserved from flies to humans, and represents an ancient strategy to evaluate the chemical composition of food.

Logic for dual TRPA1 mechanisms for sensing different levels of the same tastant

A key question concerns the logic for flies to employ both opsins and an ionotropic receptor (TRPA1) for sensing gustatory stimuli. Gustatory detection of both the lower (1 mM) and higher levels (5 mM) of aristolochic acid depends on TRPA1. 1 mM aristolochic acid, which is not very effective at directly activating TRPA1-D *in vitro*, is primarily sensed in GRNs through opsins. The *trpA1* single mutant, or *opsin* and *trpA1* double mutants showed the same reduction in action potentials in response to 1 mM aristolochic acid, indicating that the opsins function in a common pathway with TRPA1. Nevertheless, in the absence of opsins, 1 mM aristolochic acid induces a low frequency of action potentials in GRNs. This small response presumably occurs because 1 mM aristolochic acid is sufficient to elicit a minor level of direct activation of TRPA1-D.

When flies are presented with 5 mM aristolochic acid, the opsins, Gq, and PLC are dispensable. This is consistent with our finding that this higher level of aristolochic acid is sufficient to robustly activate TRPA1-D directly. At higher levels of aristolochic acid, the opsins might undergo Ca^{2+}-mediated feedback regulation, thereby attenuating their activities. Because TRPA1 is directly activated by aristolochic acid, the existence of this ionotropic mechanism for responding to aristolochic acid could provide a backup mechanism, allowing for responses to aristolochic acid at high concentrations that largely eliminate opsin activities through adaptation.

We propose that the opsin-initiated signaling cascade in GRNs provides signal amplification. In fly photoreceptor cells, light activation of a single rhodopsin leads to successive engagement of ~5 $G_{\alpha q}$ subunits, each of which stimulates one PLC [70]. The cascade culminates in activating many TRP and TRPL channels. Similarly, in fly GRNs, opsins couple to G_q, PLC, and a TRP channel (TRPA1), but only in response to lower levels of aristolochic acid. Our finding that low levels activate Rh7 in HEK293T cells supports the proposal that an opsin-initiated signaling cascade in GRNs facilitates signal amplification. This provides greater sensitivity than would be possible if direct activation of TRPA1 were the only mechanism for sensing aristolochic acid.

Archetypal role for opsins

We propose that the primordial opsins were chemosensors rather than light sensors. Chemicals sensation is ancient, and most likely preceded light sensation. We suggest that the primordial opsins bound chemicals, and these proteins were subsequently co-opted as light sensors due to interaction with a chemical ligand (retinal), which underwent a light-induced conformational change, thereby conferring light sensitivity to the opsin. Indeed, there are

primitive but extant organisms, such as comb jellies, that express many opsins in cells that do not appear to function in light sensation [71–73].

Potential roles for opsins in mammalian taste

Multiple mammalian opsins are expressed outside of the retina [73]. These include Opn3 and Opn5, which are expressed in the brain and spinal cord [74–76]. Mammalian opsins are also expressed in immune cells, liver, lungs, testis, and the aorta, although their roles are mysterious [74–79]. Moreover, although not mentioned in the text of the publications, transcriptome analyses of mammalian taste bud cells and taste organoids reveal *opsin* RNAs in these gustatory tissues [80, 81]. These results, in combination with our findings in flies, raise the exciting prospect that opsins represent a new class of taste receptor in mammalian taste buds.

STAR Methods

LEAD CONTACT AND MATERIALS AVAILABILITY

All unique/stable reagents generated in this study are available from the Lead Contact without restriction. Further information and requests for resources and reagents should be directed to and will be fulfilled by the Lead Contact, Craig Montell (cmontell@ucsb.edu).

EXPERIMENTAL MODEL AND SUBJECT DETAILS

Fly stocks—Genotypes of the fruit fly *Drosophila melanogaster* used in this study are listed in the Key Resources Table. The following lines were obtained from the Bloomington *Drosophila* Stock Center: w^{1118} (5905), $ninaE^{I17}$ (5701; referred to here as $rh1^{I17}$), $ninaE^{Df}$ [Df(3R)BSC636] (25726), $rh4^{Df}$ [Df(3L)Exel9003] (7936), $rh7^{Df}$ [Df(3L)BSC730] (26828), *rh1* RNAi (31647), *rh4* RNAi (77159), *rh7* RNAi (62176), $tubP\text{-}GAL80^{ts}$ (7018), *rh1-GAL4* (68385), *rh4-GAL4* (8627), $G_{\alpha q}{}^{1}$ or $G_{\alpha q}49B^{1}$ (42257), $G_{\alpha q}{}^{Df}$ [Df(2R)$G_{\alpha q}$1.3] (44611), $norpA^{36}$ or $norpA^{P24}$ (9048), $norpA^{Df}$ [Df(1)BSC723] (26575), $ninaD^{1}$ (42244), 15X*UAS-IVS-mCD8::GFP* (32193), *UAS-mCD8::dsRed* (27398), *40XUAS-IVSmCD8::GFP* (32195), and *Gr5a-GAL4* (57592). The following lines were provided by the indicated investigators: $rh4^{1}$, $rh5^{2}$, $rh6^{1}$, *UAS-rh1*, and *UAS-rh4* (C. Desplan), *Gr5a-I-GFP* and *Gr66-I-GFP* (K. Scott), *Gr66a-GAL4* (H. Amrein) *UAS-trpA1-C* and *UAStrpA1-D* (W.D. Tracey). The following lines were created in our laboratory and those that are available from the Bloomington *Drosophila* Stock Center are indicated with stock numbers: $rh2^{1}$, $rh3^{2}$, $rh4^{LexA}$, $rh7^{1}$ (76022), $Gr66a^{ex83}$ (25027), $Gr33a^{GAL4}$ (31425), *UASrh7* (76029), $trpA1^{1}$ (26504), $trpA1\text{-}AB^{GAL4}$ (67131), $trpA1\text{-}CD^{GAL4}$ (67134), *Gr66a-GAL4* (28801), and $UAS\text{-}rh1^{K319R}$.

Fly husbandry—Flies were raised in vials or bottles containing standard cornmeal-yeast media at 25°C in a humidified chamber under 12 hr light/12 h r dark cycles unless indicated otherwise. All mutant lines were outcrossed into the background of the control flies (w^{1118}) for five generations. Crosses for the behavior experiments were performed by placing 20–30 virgin females and 20–30 males in bottles. Other crosses were performed by placing 5–10 virgin females and 5–10 males in vials. Both females and males were used in all experiments and were selected randomly.

For behavior experiments (Figures 1, 2, 3, 4, 5, 6, 7, S1, S2, S3, and S4), 50 randomly selected flies were collected into vials one day post-eclosion, group housed, and aged until 5–7 days old. Flies were starved in 1% agarose for 18–20 hours in a humidified chamber prior to the experiment. Experiments were performed 4–6 hours after onset of light. For tip recording experiments (Figures 1, 2, 3, 4, 5, 6, 7, S1, S2, S4, S7), flies were collected into vials one day post-eclosion, group housed, and aged until 7–10 days old. For ERG experiments (Figures 3 and S3), flies were collected into vials one day post-eclosion, group housed, and aged until 5–7 days old. For carotenoid-deprived flies (Figures 3 and S3), the flies were allowed to mate on carotenoid-deficient food bottles for five days. To raise cartenoid-deficient flies, 50 randomly selected flies one day post-eclosion were collected into vials containing carotenoid-deficient food. Flies were transferred to fresh carotenoid-deficient food vials every three to four days and aged for the experiments. Flies used for immunostaining and cDNA sample preparation (Figures 4, 7, S4, and S7) were collected into vials one day post-eclosion, group housed, and aged until 5–7 days old.

Cell lines—The modified HEK293T cell line (HTLA) was obtained from the Bryan Roth laboratory. This cell line was maintained in DMEM with 10% fetal bovine serum (Thermo Fisher Scientific) and 1% Pen-Strep (Thermo Fisher Scientific) at 37°C, 80% humidity, and 5% CO_2.

METHOD DETAILS

Generating *UAS-rh1^{K319R}*—To create *UAS-rh1^{K319R}* flies we changed the codon for residue 319 from AAA to CGA, thereby resulting in a lysine to arginine substitution. To introduce this mutation in the *rh1* (*ninaE*) coding region we first amplified the wild-type cDNA from *w^{1118}* using the following primer pair: 5’-AGGGAATTGGGAATTCCAACATGGAGAGCTTTGCAGTAGC-3’ and 5’-ACAAAGATCCTCTAGATTATGCCTTGGACTCGGCC-3’. We then generated the nucleotide changes in codon 319 by amplifying the cDNA using the following primer pair: 5’-CATTTGGGGAGCTTGCTTCGCCCGATCGGCCGCCTGCTAC-3’ and 5’-CGAAGCAAGCTCCCCAAATGGTATTCAGTG-3’. We subcloned this product using InFusion (Clontech) between the EcoRI/XbaI sites of the pUAST-attB vector and injected the construct into the attP40 strain (BestGene).

Two-way choice feeding assays—Two-way choice feeding assays were performed as previously described [15] with slight modifications. 35–50 flies (aged to 5–7 days) per assay were starved in 1% agarose (Thermo Fisher Scientific) for 18–20 hours in a humidified chamber. The fly genotypes in Figures 1B and 6A were blinded to the experimenter. Flies were tested in 72-well plates (Nunc) that contained tastant/dye mixtures, and allowed to feed for 3 hours in the dark, unless indicated otherwise. The tastant/dye mixtures were added to low melting point agarose (Thermo Fisher Scientific) to avoid overheating of bitter compounds.

The preference index (PI) was calculated according to the following equation: $(N_{red} - N_{blue})/(N_{red} + N_{purple} + N_{blue})$. We determined the concentrations of the red (Sulforhodamine B; Sigma-Aldrich) and blue (Brilliant Blue FCF; Wako Chemical) food

dyes that had no significant effect on food selection by assaying the preference of control flies to each dye with 2 mM sucrose (Figures S1A–S1B). Once the concentrations were established that lead to indifference between the two food colorings, we used red dye for sucrose-only food and blue dye for food with sucrose plus bitter compound. A PI = 1.0 and −1.0 indicates complete preference for food with sucrose-only and sucrose plus bitter compound, respectively. A PI = 0 indicated no preference for either food. Trials in which <70% of the flies participated were discarded.

Extracellular tip recordings—Extracellular tip recordings were performed as previously described with slight modifications [16]. Flies aged 7–10 days were used for recordings. The fly genotypes in Figures 1D and 6C were blinded to the experimenter. Aristolochic acid was dissolved in 1 mM KCl, which served as the electrolyte, and backfilled into recording electrodes (World Precision Instruments, 1B150F-3) with 20 μm openings (Sutter Instrument, P-97 puller). Tastant-induced signals were amplified and digitalized with an IDAC-4 data acquisition device and Autospike software (Syntech). Spike sorting was used to identify spike amplitudes that correspond to the action potentials of bitter-responsive neurons. Neuronal responses were quantified by counting the number of action potentials between 200–1200 msec following contact with the stimulus.

Chemicals for feeding assays and tip recordings—The following compounds were purchased from Sigma-Aldrich: sucrose, aristolochic acid I sodium salt, and piperonyl acetate. The stock solution of aristolochic acid was dissolved in water up to 10 mM. The stock solution of piperonyl acetate was dissolved in ethanol up to 100 mM. The same amount of ethanol was added to the sucrose-only food and tastant solution to control for any behavior or electrophysiological effects of ethanol.

Cell culture and β-arrestin recruitment assay—Cell culture and the GPCR β-arrestin recruitment assay (TANGO) were performed as described [31] with minor modifications. The Rh7 coding sequence with an Nterminal FLAG tag was codon optimized, and synthesized by IDT. The construct was cloned into the TANGO vector (Addgene) at the ClaI site (FLAG::Rh7). The HTLA cells (modified HEK293T cells; a gift from the Bryan Roth laboratory) were transfected in a 6well format with Lipofectamine 2000 (Thermo Fisher Scientific) according to the manufacturer's instructions. 6–8 hours post transfection we split the cells 1:3 and replaced the media with DMEM + 2.5% fetal bovine serum (Thermo Fisher Scientific). We allowed the cells to grow for 48 hours before splitting the cells into poly-L-lysine-coated 96-well clear, flat bottom white polystyrene plates (Corning) in serum-free media. The next day drug solutions diluted in TANGO assay buffer (20 mM HEPES, 1x HBSS, pH 7.40) were added to the cells. After four hours, the medium and drug solutions were removed and replaced with 40 μL per well of BrightGlo reagent (Promega) diluted 20fold with TANGO assay buffer. We incubated the plates for 20 minutes at room temperature in the dark before measuring luminescence with a plate reader (Molecular Devices, iD3). The normalized response is calculated using following formula: RLU (relative luminescence units) = test compound RLU – average vehicle control RLU.

Aristolochic acid analogs—To identify analogs of aristolochic acid, we screened ZINC, a database of millions of purchasable compounds [82], and BitterDB, a database of bitter compounds [83]. We performed a similarity search through ZINC and BitterDB by applying a Tanimoto coefficient cutoff of 0.5 and filtered out chromophore-based derivatives in order to explore different chemical scaffolds. The remaining compounds were submitted to a 3D shape similarity screening with Phase (Schrödinger Release 2018–1, Phase, Schrödinger, LLC, New York, NY, 2018) using the aristolochic acid structure as the query. The list was narrowed to 11 compounds according to the ranking score and by visual inspection. We selected to test piperonyl acetate based on commercial availability and solubility.

Homology modeling of Rh7—We modeled the 3D structure of the Rh7 transmembrane domains by GPCR-I-TASSER, a fragment-based method in which fragments are excised from GPCR template structures and reassembled based on threading alignments [36]. The crystal structures that mostly contributed to the modeling were the human (PDB:4ZWJ), bovine (PDB:1GZM), and squid (PDB:2Z73) rhodopsins. We predicted ligand binding modes of aristolochic acid and piperonyl acetate to Rh7 using Induced Fit Docking (Schrödinger Release 2018–1, Induced Fit Docking protocol; Glide, Schrödinger, LLC, New York, NY, 2018; Prime, Schrödinger, LLC, New York, NY, 2018). The grid box was centroid to the retinal coordinates in bovine rhodopsin. The docking was performed using the Standard Precision (SP) mode of Glide (Table S2).

Quantitative PCR—To detect expression of *opsin* mRNAs in the head and labellum by reverse transcription PCR (RT-PCR) and quantitative PCR (RT-qPCR) we isolated RNA from 5 heads without labella, and 25 labella using TRIzol (Thermo Fisher Scientific). We prepared cDNA using SuperScript III Reverse Transcriptase (Thermo Fisher Scientific) with oligodT primers. For RT-PCR, we amplified for 40 cycles using Phusion DNA polymerase (New England BioLabs) and for RT-qPCR, we amplified for 50 cycles using the LightCycler 480 SYBR Green I Master Mix (Roche). *rh1*, 5’- CTTGTCCACCACCGATCCA-3’ and 5’-TGACGCAGCCAGTAACCAAA-3’ (103 bp); *rh4*, 5’- TCACCAAGGCGGTGATAATG-3’ and 5’-CGAAAGATAGTCGAAGGAGCAG-3’ (134 bp); *rh7*, 5’-GGCAATGTAGCTCAGGTCGT-3’ and 5’CGCTGTGAATGTAGGCAAGG-3’ (127 bp); and *α-tubulin*, 5’-TGTCGCGTGTGAAACACTTC-3’ and 5’-AGCAGGCGTTTCCAATCTG-3’ (96 bp).

Immunostaining—Labella: Dissected labella from 5–7-day old adult flies were fixed in 4% paraformaldehyde in PBST (PBS + 0.5% Triton X-100) for 30 min at room temperature. Samples were washed in PBST (10 min, 3 times) and blocked with 5% normal goat serum (MP Biomedicals) in PBST (block buffer) for 30 min at room temperature, followed by incubation with primary antibodies in blocking buffer for 1–3 days at 10°C. The samples were washed with PBST (10 min, 3 times) and incubated with the secondary antibodies in blocking buffer overnight at 4°C in the dark. After a final PBST wash (10 min, 3 times), the samples were mounted using Vectashield (Vector Laboratory, H-1000) and a coverslip was secured with nail polish. The samples were imaged using a Zeiss LSM 700 confocal laser scanning microscope using a 20x/0.8 Plan-Apochromat DIC objective. The images were processed using Zen software and ImageJ. The following primary and secondary antibodies

were used at the indicated dilutions: chicken anti-GFP (1:200; Thermo Fisher Scientific), rabbit anti-DsRed (1:500; Clontech), AlexaFluor 488 goat anti-chicken IgG (1:1000; Thermo Fisher Scientific), AlexaFluor 568 goat anti-rabbit IgG (1:1000; Thermo Fisher Scientific).

Cell culture: Cells were plated at a density of 40,000 cells per well onto 7 mm coverslips (Warner Instruments) in 24-well plates a few hours before fixation. For permeabilized cells, the procedure was as stated above. For non-permeabilized cells, Triton X-100 was omitted. The samples were mounted using Vectashield with DAPI (Vector Laboratory, H-1500). The following primary and secondary antibodies were used at the indicated dilutions: rabbit anti-FLAG (1:500; Sigma-Aldrich), AlexaFluor 488 goat anti-rabbit IgG (1:1000; Thermo Fisher Scientific).

Recipe for carotenoid-deficient food—The carotenoid-deficient food was comprised of the following ingredients: 40 mg/mL dry yeast (Genesee Scientific), 40 mg/mL D-(+)-glucose (Sigma-Aldrich), 48 mg/mL rice powder (United Foodstuff Company), 8 mg/mL agar (BD Diagnostics), 0.24 mg/mL cholesterol (Sigma-Aldrich), 3.6 mg/mL methyl 4-hydroxybenzoate (Sigma-Aldrich), and 0.32% (v/v) propionic acid (Sigma-Aldrich).

Electroretinogram recordings—Electroretinogram recordings were performed as previously described [84] with slight modifications. Briefly, two glass electrodes filled with Ringer's solution were inserted into small drops of electrode cream placed on the surfaces of the compound eye and the thorax. Flies were exposed to 10 sec of orange light (Klinger Educational Products, 580 nm filter). Light-induced signals were amplified using an IE-210 amplifier (Warner Instruments) and the data were acquired with a Powerlab 4/30 device and LabChart 6 software (AD Instruments).

Two-electrode voltage clamp recordings—We subcloned the *trpA1-C* and *trpA1-D* cDNAs (referred to as *trpA1-RH* and *trpA1-RG* in FlyBase) into the NotI site of the pCS2-MT vector (Addgene), and synthesized cRNAs using the mMESSAGE mMACHINE SP6 transcription kit (Thermo Fisher Scientific). We surgically removed oocytes from *Xenopus laevis* and maintained them in OR3 medium (50% (v/v) L-15 Leibovitz's medium (Thermo Fisher Scientific), 15 mM HEPES, 0.1 mg/mL Gentamicin (Sigma-Aldrich), 0.2% (v/v) Fungizone (Sigma-Aldrich), 100 μg/mL penicillin/streptomycin, pH 7.5) for 24 hours at 18°C before injecting them with ~40 ng cRNA using a micro-injector (Nanoject, Drummond Scientific). We allowed the injected oocytes to recover for 48 hours in OR3 medium at 18°C before performing the recordings. We held the oocytes at −40 mV and recorded the whole-cell currents before and after chemical perfusion. We diluted the chemicals in Ca^{2+}- and Mg^{2+}-free ND96 buffer (96 mM NaCl, 2 mM KCl, 5 mM HEPES, pH 7.5) to minimize precipitation of aristolochic acid.

QUANTIFICATION AND STATISTICAL ANALYSIS

All error bars represent standard error of the mean (SEM). The number of times each experiment was repeated (n) are indicated in the figure legends. For the two-way choice assays each "n" represents a single test performed with 35–50 animals. Each "n" for the tip

recordings represents an analysis of a single, independent fly. Each “n” for the ERGs represents an analysis of a single, independent fly. For RT-qPCR experiments, the data are represented as the mean of three independent experiments. For the β-arrestin recruitment assay, the data are represented as the mean of four independent experiments. All graphs were generated using Prism 7 (Graphpad).

For behavior and electrophysiology (tip recording) experiments, we estimated the sample size using preliminary data obtained with control (w^{1118}) and $rh1^{I17}$ mutant flies ($ninaE^{I17}$) flies with an n=5. We set the significance level, α=0.05 and power, 1-β=0.9. For sample size calculations, we assumed that the preliminary data follow a normal distribution. The power calculator estimated n=8 for the two-way choice assay and n=12 for the tip recordings.

We tested each data set for normality using the Shapiro-Wilk test. For parametric tests, we used the unpaired Student’s *t*-test and the one-way ANOVA with Tukey’s multiple comparisons test. For non-parametric tests, we used the Mann-Whitney test and the Kruskal-Wallis test with Dunn’s multiple comparisons test. The statistical test used are indicated in the figure legends. Statistical tests were performed using Prism 7 (Graphpad). Asterisks indicate statistical significance, where * indicates $p<0.05$, ** indicates $p<0.01$, and *** indicates $p<0.001$.

Supplementary Material

Refer to Web version on PubMed Central for supplementary material.

Acknowledgments

We thank Wesley Kroeze and Bryan Roth for providing HTLA cells and guidance for the TANGO assay, and Chao Liu for conducting preliminary studies. NYL was partially supported by a predoctoral fellowship from the National Eye Institute (F31EY027191). MYN received an ISF grant (494/16). This work was supported by grants to CM from the National Institute on Deafness and Other Communication Disorders (DC007864 and DC016278).

References

1. Liman ER, Zhang YV, and Montell C. (2014). Peripheral coding of taste. Neuron 81, 984–1000. [PubMed: 24607224]
2. Zhang Y, Hoon MA, Chandrashekar J, Mueller KL, Cook B, Wu D, Zuker CS, and Ryba NJ (2003). Coding of sweet, bitter, and umami tastes: different receptor cells sharing similar signaling pathways. Cell 112, 293–301. [PubMed: 12581520]
3. Pérez CA, Huang L, Rong M, Kozak JA, Preuss AK, Zhang H, Max M, and Margolskee RF (2002). A transient receptor potential channel expressed in taste receptor cells. Nat. Neurosci 5, 1169–1176. [PubMed: 12368808]
4. Damak S, Rong M, Yasumatsu K, Kokrashvili Z, Perez CA, Shigemura N, Yoshida R, Mosinger B Jr., Glendinning JI, Ninomiya Y, et al. (2006). Trpm5 null mice respond to bitter, sweet, and umami compounds. Chem. Senses 31, 253–264. [PubMed: 16436689]
5. Dutta Banik D, Martin LE, Freichel M, Torregrossa AM, and Medler KF (2018). TRPM4 and TRPM5 are both required for normal signaling in taste receptor cells. Proc. Natl. Acad. Sci. U. S. A 115, E772–E781. [PubMed: 29311301]
6. Kim SH, Lee Y, Akitake B, Woodward OM, Guggino WB, and Montell C. (2010). *Drosophila* TRPA1 channel mediates chemical avoidance in gustatory receptor neurons. Proc. Natl. Acad. Sci. USA 107, 8440–8445. [PubMed: 20404155]
7. Kühne W. (1878). On the stable colours of the retina. J. Physiol 1, 109–212 105.

8. Boll F. (1877). Zur anatomie und physiologie der retina. Anat. u. Physiol 1877, 4–36.
9. Boll F. (1977). On the anatomy and physiology of the retina. Vision Res. 17, 1249–1265. [PubMed: 345608]
10. Costanzi S, Siegel J, Tikhonova IG, and Jacobson KA (2009). Rhodopsin and the others: a historical perspective on structural studies of G protein-coupled receptors. Curr. Pharm. Des 15, 3994–4002. [PubMed: 20028316]
11. Zanini D, Giraldo D, Warren B, Katana R, Andres M, Reddy S, Pauls S, Schwedhelm-Domeyer N, Geurten BRH, and Gopfert MC (2018). Proprioceptive opsin functions in *Drosophila* larval locomotion. Neuron 98, 67–74. [PubMed: 29551493]
12. Senthilan PR, Piepenbrock D, Ovezmyradov G, Nadrowski B, Bechstedt S, Pauls S, Winkler M, Mobius W, Howard J, and Göpfert MC (2012). *Drosophila* auditory organ genes and genetic hearing defects. Cell 150, 10421054.
13. Sokabe T, Chen HS, Luo J, and Montell C. (2016). A switch in thermal preference in *Drosophila* larvae depends on multiple rhodopsins. Cell Rep. 17, 336–344. [PubMed: 27705783]
14. Shen WL, Kwon Y, Adegbola AA, Luo J, Chess A, and Montell C. (2011). Function of rhodopsin in temperature discrimination in *Drosophila*. Science 331, 1333–1336. [PubMed: 21393546]
15. Lee Y, Kim SH, and Montell C. (2010). Avoiding DEET through insect gustatory receptors. Neuron 67, 555–561. [PubMed: 20797533]
16. Moon SJ, Köttgen M, Jiao Y, Xu H, and Montell C. (2006). A taste receptor required for the caffeine response in vivo. Curr. Biol 16, 1812–1817. [PubMed: 16979558]
17. Moon SJ, Lee Y, Jiao Y, and Montell C. (2009). A *Drosophila* gustatory receptor essential for aversive taste and inhibiting male-to-male courtship. Curr. Biol 19, 1623–1627. [PubMed: 19765987]
18. Sung HY, Jeong YT, Lim JY, Kim H, Oh SM, Hwang SW, Kwon JY, and Moon SJ (2017). Heterogeneity in the Drosophila gustatory receptor complexes that detect aversive compounds. Nat Commun 8, 1484. [PubMed: 29133786]
19. Weiss LA, Dahanukar A, Kwon JY, Banerjee D, and Carlson JR (2011). The molecular and cellular basis of bitter taste in *Drosophila*. Neuron 69, 258–272. [PubMed: 21262465]
20. Dunipace L, Meister S, McNealy C, and Amrein H. (2001). Spatially restricted expression of candidate taste receptors in the *Drosophila* gustatory system. Curr. Biol 11, 822–835. [PubMed: 11516643]
21. Montell C. (2012). *Drosophila* visual transduction. Trends Neurosci. 35, 356–363. [PubMed: 22498302]
22. Ni JD, Baik LS, Holmes TC, and Montell C. (2017). A rhodopsin in the brain functions in circadian photoentrainment in *Drosophila*. Nature 545, 340344.
23. Harris WA, Ready DF, Lipson ED, Hudspeth AJ, and Stark WS (1977). Vitamin A deprivation and *Drosophila* photopigments. Nature 266, 648–650. [PubMed: 404571]
24. Ozaki K, Nagatani H, Ozaki M, and Tokunaga F. (1993). Maturation of major Drosophila rhodopsin, ninaE, requires chromophore 3-hydroxyretinal. Neuron 10, 1113–1119. [PubMed: 8318232]
25. Kiefer C, Sumser E, Wernet MF, and Von Lintig J. (2002). A class B scavenger receptor mediates the cellular uptake of carotenoids in *Drosophila*. Proc. Natl. Acad. Sci. USA 99, 10581–10586. [PubMed: 12136129]
26. Wang T, Jiao Y, and Montell C. (2007). Dissection of the pathway required for generation of vitamin A and for *Drosophila* phototransduction. J. Cell Biol 177, 305–316. [PubMed: 17452532]
27. Johnson EC, and Pak WL (1986). Electrophysiological study of *Drosophila* rhodopsin mutants. J. Gen. Physiol 88, 651–673. [PubMed: 3097245]
28. Wang JK, McDowell JH, and Hargrave PA (1980). Site of attachment of 11*cis*-retinal in bovine rhodopsin. Biochemistry 19, 5111–5117. [PubMed: 6450610]
29. Zuker CS, Cowman AF, and Rubin GM (1985). Isolation and structure of a rhodopsin gene from D. melanogaster. Cell 40, 851–858. [PubMed: 2580638]
30. O'Tousa JE, Baehr W, Martin RL, Hirsh J, Pak WL, and Applebury ML (1985). The Drosophila *ninaE* gene encodes an opsin. Cell 40, 839–850. [PubMed: 2985266]

31. Kroeze WK, Sassano MF, Huang XP, Lansu K, McCorvy JD, Giguere PM, Sciaky N, and Roth BL (2015). PRESTO-Tango as an open-source resource for interrogation of the druggable human GPCRome. Nat. Struct. Mol. Biol 22, 362–369. [PubMed: 25895059]
32. Burdock GA (2009). Fenaroli's Handbook of Flavor Ingredients, 6th Edition, (Milton Park: Taylor & Francis).
33. Kain P, Badsha F, Hussain SM, Nair A, Hasan G, and Rodrigues V. (2010). Mutants in phospholipid signaling attenuate the behavioral response of adult *Drosophila* to trehalose. Chem. Senses 35, 663–673. [PubMed: 20543015]
34. Masek P, and Keene AC (2013). *Drosophila* fatty acid taste signals through the PLC pathway in sugar-sensing nurons. PLoS Genet. 9, e1003710. [PubMed: 24068941]
35. Thorne N, Chromey C, Bray S, and Amrein H. (2004). Taste perception and coding in *Drosophila*. Curr. Biol 14, 1065–1079. [PubMed: 15202999]
36. Zhang J, Yang J, Jang R, and Zhang Y. (2015). GPCR-I-TASSER: a hybrid approach to G protein-coupled receptor structure modeling and the application to the human genome. Structure 23, 1538–1549. [PubMed: 26190572]
37. Bloomquist BT, Shortridge RD, Schneuwly S, Perdew M, Montell C, Steller H, Rubin G, and Pak WL (1988). Isolation of a putative phospholipase C gene of Drosophila, *norpA*, and its role in phototransduction. Cell 54, 723–733. [PubMed: 2457447]
38. Hardie RC, and Minke B. (1992). The *trp* gene is essential for a light-activated Ca^{2+} channel in Drosophila photoreceptors. Neuron 8, 643–651. [PubMed: 1314617]
39. Montell C, and Rubin GM (1989). Molecular characterization of the Drosophila *trp* locus: a putative integral membrane protein required for phototransduction. Neuron 2, 1313–1323. [PubMed: 2516726]
40. Niemeyer BA, Suzuki E, Scott K, Jalink K, and Zuker CS (1996). The Drosophila light-activated conductance is composed of the two channels TRP and TRPL. Cell 85, 651–659. [PubMed: 8646774]
41. Scott K, Becker A, Sun Y, Hardy R, and Zuker C. (1995). $G_{q\alpha}$ protein function in vivo: genetic dissection of its role in photoreceptor cell physiology. Neuron 15, 919–927. [PubMed: 7576640]
42. Meunier N, Marion-Poll F, Rospars JP, and Tanimura T. (2003). Peripheral coding of bitter taste in *Drosophila*. J. Neurobiol 56, 139–152. [PubMed: 12838579]
43. Jeong YT, Shim J, Oh SR, Yoon H,I, Kim CH, Moon SJ, and Montell C(2013). An Odorant-Binding Protein required for suppression of sweet taste by bitter chemicals. Neuron 79, 725–737. [PubMed: 23972598]
44. Chu B, Chui V, Mann K, and Gordon MD (2014). Presynaptic gain control drives sweet and bitter taste integration in *Drosophila*. Curr. Biol 24, 1978–1984 [PubMed: 25131672]
45. Zhong L, Bellemer A, Yan H, Honjo K, Robertson J, Hwang RY, Pitt GS, and Tracey WD (2012). Thermosensory and non-thermosensory isoforms of *Drosophila melanogaster* TRPA1 reveal heat sensor domains of a thermoTRP channel. Cell Rep. 1, 43–55. [PubMed: 22347718]
46. Kwon Y, Shim HS, Wang X, and Montell C. (2008). Control of thermotactic behavior via coupling of a TRP channel to a phospholipase C signaling cascade. Nat. Neurosci 11, 871–873. [PubMed: 18660806]
47. Luo J, Shen WL, and Montell C. (2017). TRPA1 mediates sensation of the rate of temperature change in *Drosophila* larvae. Nat. Neurosci 20, 34–41. [PubMed: 27749829]
48. Kang K, Panzano VC, Chang EC, Ni L, Dainis AM, Jenkins AM, Regna K, Muskavitch MA, and Garrity PA (2012). Modulation of TRPA1 thermal sensitivity enables sensory discrimination in *Drosophila*. Nature 481, 7680.
49. Bandell M, Story GM, Hwang SW, Viswanath V, Eid SR, Petrus MJ, Earley TJ, and Patapoutian A. (2004). Noxious cold ion channel TRPA1 is activated by pungent compounds and bradykinin. Neuron 41, 849–857. [PubMed: 15046718]
50. Jordt SE, Bautista DM, Chuang HH, McKemy DD, Zygmunt PM, Högestätt ED, Meng ID, and Julius D. (2004). Mustard oils and cannabinoids excite sensory nerve fibres through the TRP channel ANKTM1. Nature 427, 260–265. [PubMed: 14712238]

51. Kang K, Pulver SR, Panzano VC, Chang EC, Griffith LC, Theobald DL, and Garrity PA (2010). Analysis of *Drosophila* TRPA1 reveals an ancient origin for human chemical nociception. Nature 464, 597–600. [PubMed: 20237474]
52. Katana R, Guan C, Zanini D, Larsen ME, Giraldo D, Geurten BRH, Schmidt CF, Britt SG, and Gopfert MC (2019). Chromophore-independent roles of opsin apoproteins in *Drosophila* mechanoreceptors. Curr. Biol
53. Mazzoni EO, Celik A, Wernet MF, Vasiliauskas D, Johnston RJ, Cook TA, Pichaud F, and Desplan C. (2008). *Iroquois complex* genes induce coexpression of *rhodopsins* in *Drosophila*. PLoS Biol. 6, e97. [PubMed: 18433293]
54. Hu X, Leming MT, Whaley MA, and O'Tousa JE (2014). Rhodopsin coexpression in UV photoreceptors of *Aedes aegypti* and *Anopheles gambiae* mosquitoes. J. Exp. Biol 217, 1003–1008. [PubMed: 24311804]
55. Applebury ML, Antoch MP, Baxter LC, Chun LL, Falk JD, Farhangfar F, Kage K, Krzystolik MG, Lyass LA, and Robbins JT (2000). The murine cone photoreceptor: a single cone type expresses both S and M opsins with retinal spatial patterning. Neuron 27, 513–523. [PubMed: 11055434]
56. Fotiadis D, Jastrzebska B, Philippsen A, Muller DJ, Palczewski K, and Engel A. (2006). Structure of the rhodopsin dimer: a working model for Gprotein-coupled receptors. Curr. Opin. Struct. Biol 16, 252–259. [PubMed: 16567090]
57. Rivero-Muller A, Jonas KC, Hanyaloglu AC, and Huhtaniemi I. (2013). Di/oligomerization of GPCRs-mechanisms and functional significance. Prog. Mol. Biol. Transl. Sci 117, 163–185. [PubMed: 23663969]
58. Franco R, Martinez-Pinilla E, Lanciego JL, and Navarro G. (2016). Basic pharmacological and structural Evidence for class A G-protein-coupled receptor heteromerization. Front. Pharmacol 7, 76. [PubMed: 27065866]
59. Damian M, Pons V, Renault P, M'Kadmi C, Delort B, Hartmann L, Kaya AI, Louet M, Gagne D, Ben Haj Salah K, et al. (2018). GHSR-D2R heteromerization modulates dopamine signaling through an effect on G protein conformation. Proc. Natl. Acad. Sci. U. S. A 115, 4501–4506. [PubMed: 29632174]
60. Lambert NA (2010). GPCR dimers fall apart. Sci Signal 3, pe12. [PubMed: 20354223]
61. Redka DS, Morizumi T, Elmslie G, Paranthaman P, Shivnaraine RV, Ellis J, Ernst OP, and Wells JW (2014). Coupling of G proteins to reconstituted monomers and tetramers of the M_2 muscarinic receptor. J. Biol. Chem 289, 24347–24365. [PubMed: 25023280]
62. Petrin D, and Hebert TE (2012). The functional size of GPCRs - monomers, dimers or tetramers? Subcell. Biochem 63, 67–81. [PubMed: 23161133]
63. Navarro G, Cordomi A, Zelman-Femiak M, Brugarolas M, Moreno E, Aguinaga D, Perez-Benito L, Cortes A, Casado V, Mallol J, et al. (2016). Quaternary structure of a G-protein-coupled receptor heterotetramer in complex with G_i and G_s. BMC Biol. 14, 26. [PubMed: 27048449]
64. Cordomi A, Navarro G, Aymerich MS, and Franco R. (2015). Structures for G-protein-coupled receptor tetramers in complex with G proteins. Trends Biochem. Sci 40, 548–551. [PubMed: 26410595]
65. Sleno R, and Hebert TE (2019). Shaky ground - The nature of metastable GPCR signalling complexes. Neuropharmacology.
66. Yarmolinsky DA, Zuker CS, and Ryba NJ (2009). Common sense about taste: from mammals to insects. Cell 139, 234–244. [PubMed: 19837029]
67. Adler E, Hoon MA, Mueller KL, Chandrashekar J, Ryba NJ, and Zuker CS (2000). A novel family of mammalian taste receptors. Cell 100, 693–702. [PubMed: 10761934]
68. Mueller KL, Hoon MA, Erlenbach I, Chandrashekar J, Zuker CS, and Ryba NJ (2005). The receptors and coding logic for bitter taste. Nature 434, 225–229. [PubMed: 15759003]
69. Meyerhof W, Batram C, Kuhn C, Brockhoff A, Chudoba E, Bufe B, Appendino G, and Behrens M. (2010). The molecular receptive ranges of human TAS2R bitter taste receptors. Chem. Senses 35, 157–170. [PubMed: 20022913]
70. Yau KW, and Hardie RC (2009). Phototransduction motifs and variations. Cell 139, 246–264. [PubMed: 19837030]

71. Feuda R, Rota-Stabelli O, Oakley TH, and Pisani D. (2014). The comb jelly opsins and the origins of animal phototransduction. Genome Biol. Evol 6, 1964–1971. [PubMed: 25062921]
72. Suga H, Schmid V, and Gehring WJ (2008). Evolution and functional diversity of jellyfish opsins. Curr. Biol 18, 51–55. [PubMed: 18160295]
73. Leung NY, and Montell C. (2017). Unconventional roles of opsins. Annu Rev Cell Dev Biol 33, 241–264. [PubMed: 28598695]
74. Blackshaw S, and Snyder SH (1999). Encephalopsin: a novel mammalian extraretinal opsin discretely localized in the brain. J. Neurosci 19, 3681–3690. [PubMed: 10234000]
75. Halford S, Freedman MS, Bellingham J, Inglis SL, Poopalasundaram S, Soni BG, Foster RG, and Hunt DM (2001). Characterization of a novel human opsin gene with wide tissue expression and identification of embedded and flanking genes on chromosome 1q43. Genomics 72, 203–208. [PubMed: 11401433]
76. Kumbalasiri T, and Provencio I. (2005). Melanopsin and other novel mammalian opsins. Exp. Eye Res 81, 368–375. [PubMed: 16005867]
77. Sikka G, Hussmann GP, Pandey D, Cao S, Hori D, Park JT, Steppan J, Kim JH, Barodka V, Myers AC, et al. (2014). Melanopsin mediates lightdependent relaxation in blood vessels. Proc. Natl. Acad. Sci. USA
78. Tarttelin EE, Bellingham J, Hankins MW, Foster RG, and Lucas RJ (2003). Neuropsin (Opn5): a novel opsin identified in mammalian neural tissue. FEBS Lett. 554, 410–416. [PubMed: 14623103]
79. White JH, Chiano M, Wigglesworth M, Geske R, Riley J, White N, Hall S, Zhu G, Maurio F, Savage T, et al. (2008). Identification of a novel asthma susceptibility gene on chromosome 1qter and its functional evaluation. Hum. Mol. Genet 17, 1890–1903. [PubMed: 18344558]
80. Sukumaran SK, Lewandowski BC, Qin Y, Kotha R, Bachmanov AA, and Margolskee RF (2017). Whole transcriptome profiling of taste bud cells. Sci. Rep 7, 7595. [PubMed: 28790351]
81. Ren W, Aihara E, Lei W, Gheewala N, Uchiyama H, Margolskee RF, Iwatsuki K, and Jiang P. (2017). Transcriptome analyses of taste organoids reveal multiple pathways involved in taste cell generation. Sci. Rep 7, 4004. [PubMed: 28638111]
82. Sterling T, and Irwin JJ (2015). ZINC 15—ligand discovery for everyone. J. Chem. Inf. Model 55, 2324–2337. [PubMed: 26479676]
83. Dagan-Wiener A, Di Pizio A, Nissim I, Bahia MS, Dubovski N, Margulis E, and Niv MY (2019). BitterDB: taste ligands and receptors database in 2019. Nucleic Acids Res. 47, D1179–D1185. [PubMed: 30357384]
84. Wes PD, Xu X-ZS, Li H-S, Chien F, Doberstein SK, and Montell C. (1999). Termination of phototransduction requires binding of the NINAC myosin III and the PDZ protein INAD. Nat. Neurosci 2, 447–453. [PubMed: 10321249]
85. Vasiliauskas D, Mazzoni EO, Sprecher SG, Brodetskiy K, Johnston RJ Jr, Lidder P, Vogt N, Celik A, and Desplan C. (2011). Feedback from rhodopsin controls rhodopsin exclusion in *Drosophila* photoreceptors. Nature 479, 108–112. [PubMed: 21983964]
86. Yamaguchi S, Wolf R, Desplan C, and Heisenberg M. (2008). Motion vision is independent of color in *Drosophila*. Proc. Natl. Acad. Sci. USA 105, 49104915.
87. Fischler W, Kong P, Marella S, and Scott K. (2007). The detection of carbonation by the *Drosophila* gustatory system. Nature 448, 1054–1057. [PubMed: 17728758]
88. Bischof J, Maeda RK, Hediger M, Karch F, and Basler K. (2007). An optimized transgenesis system for *Drosophila* using germ-line-specific ΦC31 integrases. Proc. Natl. Acad. Sci. USA 104, 3312–3317. [PubMed: 17360644]

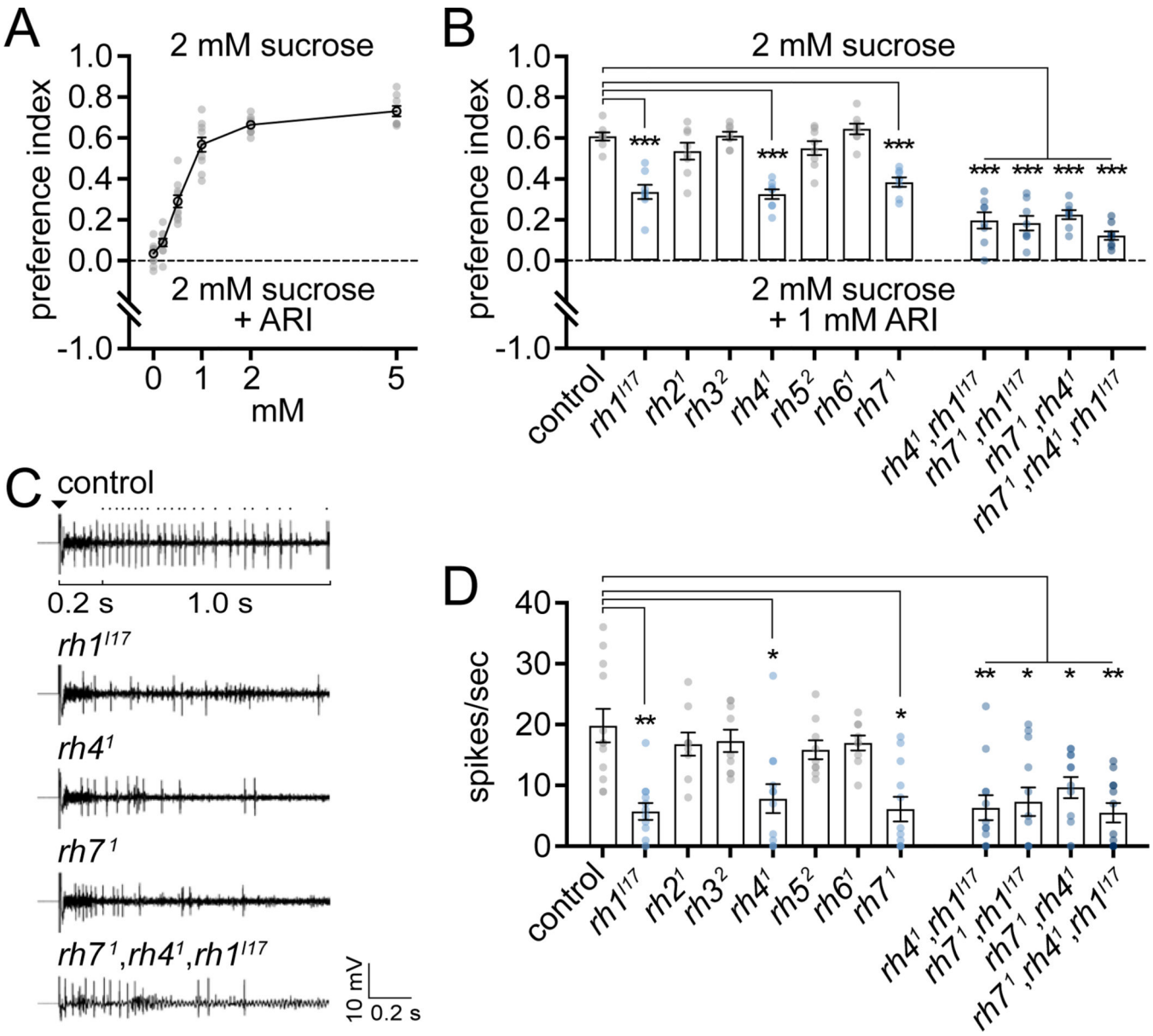

Figure 1. Fly avoidance of aristolochic acid requires Rh1, Rh4, and Rh7

(A) Two-way choice feeding assays testing preferences of control (w^{1118}) flies for 2 mM sucrose versus 2 mM sucrose plus the indicated concentrations of aristolochic acid (ARI). n=8–10 for each concentration. Means ±SEMs. See also Figures S1A and S1B.

(B) Two-way choice feeding assays testing preferences of *opsin* mutants for 2 mM sucrose versus 2 mM sucrose plus 1 mM ARI. n=8 per genotype. Means ±SEMs. Statistics performed using one-way ANOVA with Tukey's multiple comparisons test. See also Figure S1D and Table S1.

(C) Representative tip recording traces by stimulating S6 sensilla of the indicated flies with 1 mM ARI (arrowhead indicates contact of the sensillum with the electrode). The larger amplitudes spikes are ARI-induced action potentials. Dots above the control trace denote the counted spikes between 200–1200 msec following contact.

(D) Quantification of tip recording action potentials between 200–1200 msec following application of 1 mM ARI. n=9–12 per genotype. Means ±SEMs. Statistics performed using Kruskal-Wallis test with Dunn's multiple comparisons test. See also Figures S1E, S1G, and S1H, and Table S1.

* $p<0.05$, ** $p<0.01$, and *** $p<0.001$.

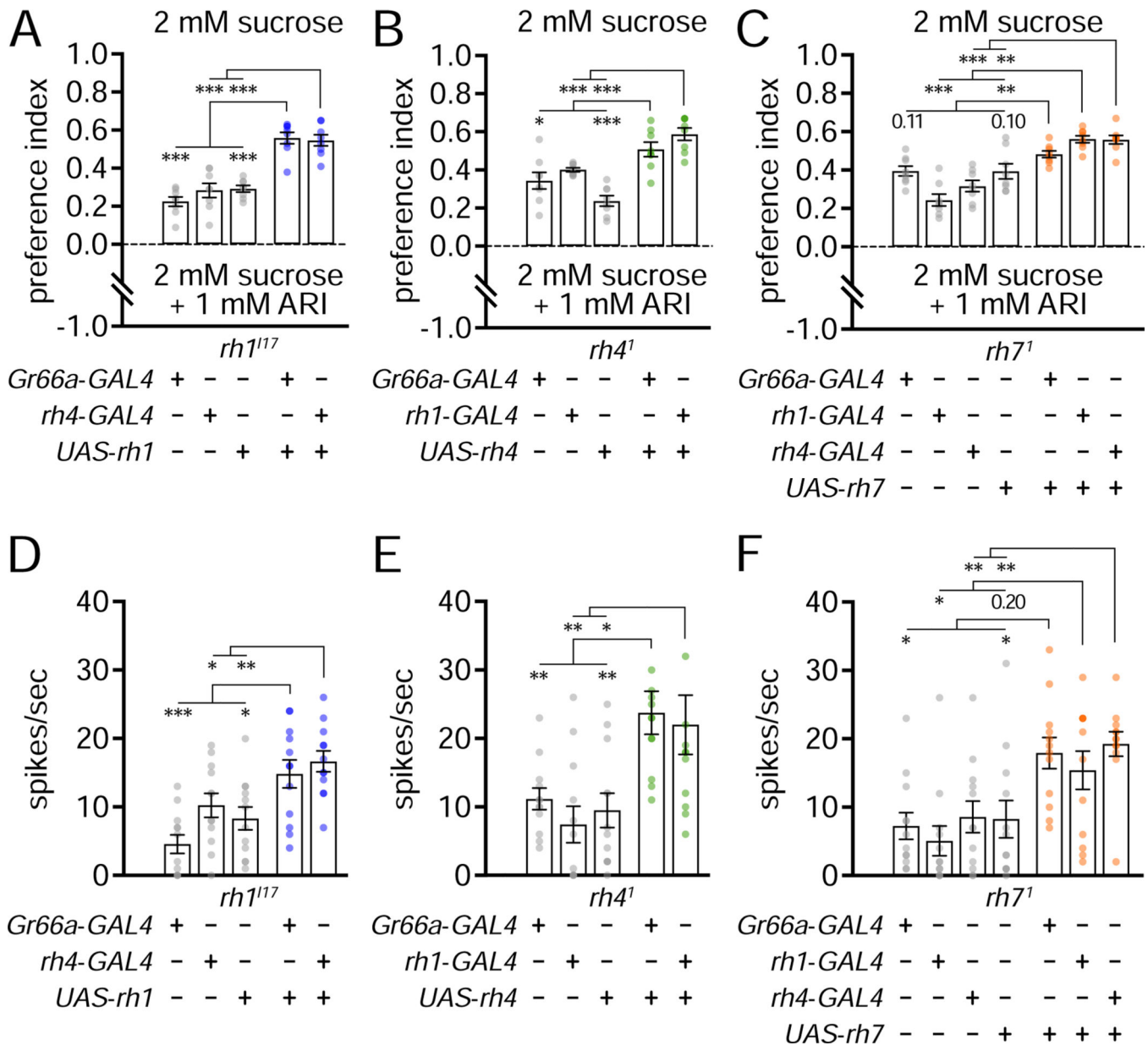

Figure 2. Requirements for opsins in GRNs for detecting aristolochic acid

(A–C) Two-way choice feeding assays testing the preferences for 2 mM sucrose versus 2 mM sucrose plus 1 mM aristolochic acid (ARI). n=8 per genotype. Means ±SEMs. Statistics performed using one-way ANOVA with Tukey's multiple comparisons test.

(D–F) Quantification of tip recording action potentials of the indicated flies between 200–1200 msec following application of 1 mM ARI. n=12 per genotype. Means ±SEMs. Statistics performed using the Kruskal-Wallis test with Dunn's multiple comparisons test. See also Figures S2A–S2C.

(A,D) Rescue of the *rh1*^{I17} mutant **(A)** behavioral and **(D)** electrophysiological phenotypes by expressing *UAS-rh1* using the indicated *GAL4*.

(B,E) Rescue of *rh4*^{1} mutant **(B)** behavioral and **(E)** electrophysiological phenotypes by expressing *UAS-rh4* using the indicated *GAL4*.
(C,F) Rescue of *rh7*^{1} mutant **(C)** behavioral and **(F)** electrophysiological phenotypes by expressing *UAS-rh7* using the indicated *GAL4*.
* $p<0.05$, ** $p<0.01$, and *** $p<0.001$.

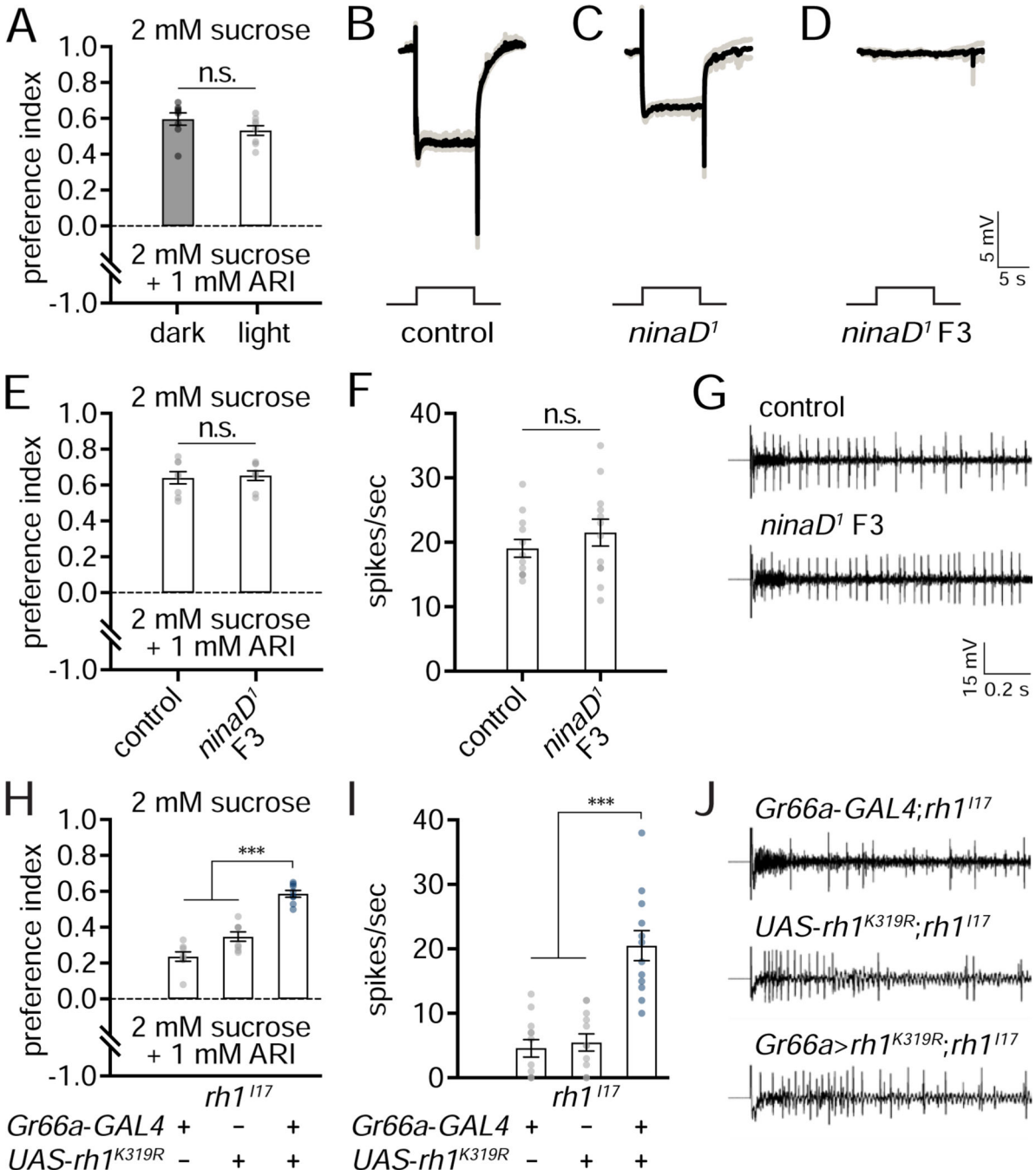

Figure 3. Chromophore is dispensable for opsin-mediated chemosensation

(A) Light does not significantly affect ARI repulsion. Two-way choice feeding assays testing the preferences of control (w^{1118}) flies for 2 mM sucrose versus 2 mM sucrose plus 1 mM aristolochic acid (ARI) in the dark (gray) versus light (white). n=8 per condition. Means ±SEMs. Statistics performed using the unpaired Student's *t*-test.

(B–D) Electroretinogram recordings of **(B)** control and **(C)** *ninaD*^{1} flies reared on standard food, and **(D)** *ninaD*^{1} flies reared on carotenoid-deficient food for three generations (F3).

The flies were exposed to a 10 sec light pulse. The black trace represents the mean and the gray traces represent ±SEMs. n=4 per condition. See also Figures S3B and S3C.

(E) Two-way choice feeding assays testing the preferences of control and *ninaD*^{1} F3 flies for 2 mM sucrose versus 2 mM sucrose plus 1 mM ARI. n=8 per genotype. Means±SEMs. Statistics were performed using the unpaired Student's *t*-test.

(F) Quantification of tip recording action potentials of control and *ninaD*^{1} F3 flies between 200–1200 msec following application of 1 mM ARI. n=12 per genotype. Means ±SEMs. Statistics were performed using the unpaired Student's *t*-test.

(G) Representative tip recording traces (Figure 3F) by stimulating S6 sensilla with 1 mM ARI.

(H,I) Rescue of *rh1*^{I17} phenotype by expressing *UAS-rh1*^{K319R} using the *Gr66a-GAL4*. **(H)** Two-way choice feeding assays testing the preferences for 2 mM sucrose versus 2 mM sucrose plus 1 mM ARI. n=8 per genotype. **(I)** Quantification of tip recording action potentials between 200–1200 msec following application of 1 mM ARI. n=12 per genotype. Means ±SEMs. Statistics were performed using one-way ANOVA with Tukey's multiple comparisons test.

(J) Representative tip recording traces (Figure 3I) by stimulating S6 sensilla with 1 mM ARI.

*** $p<0.001$.

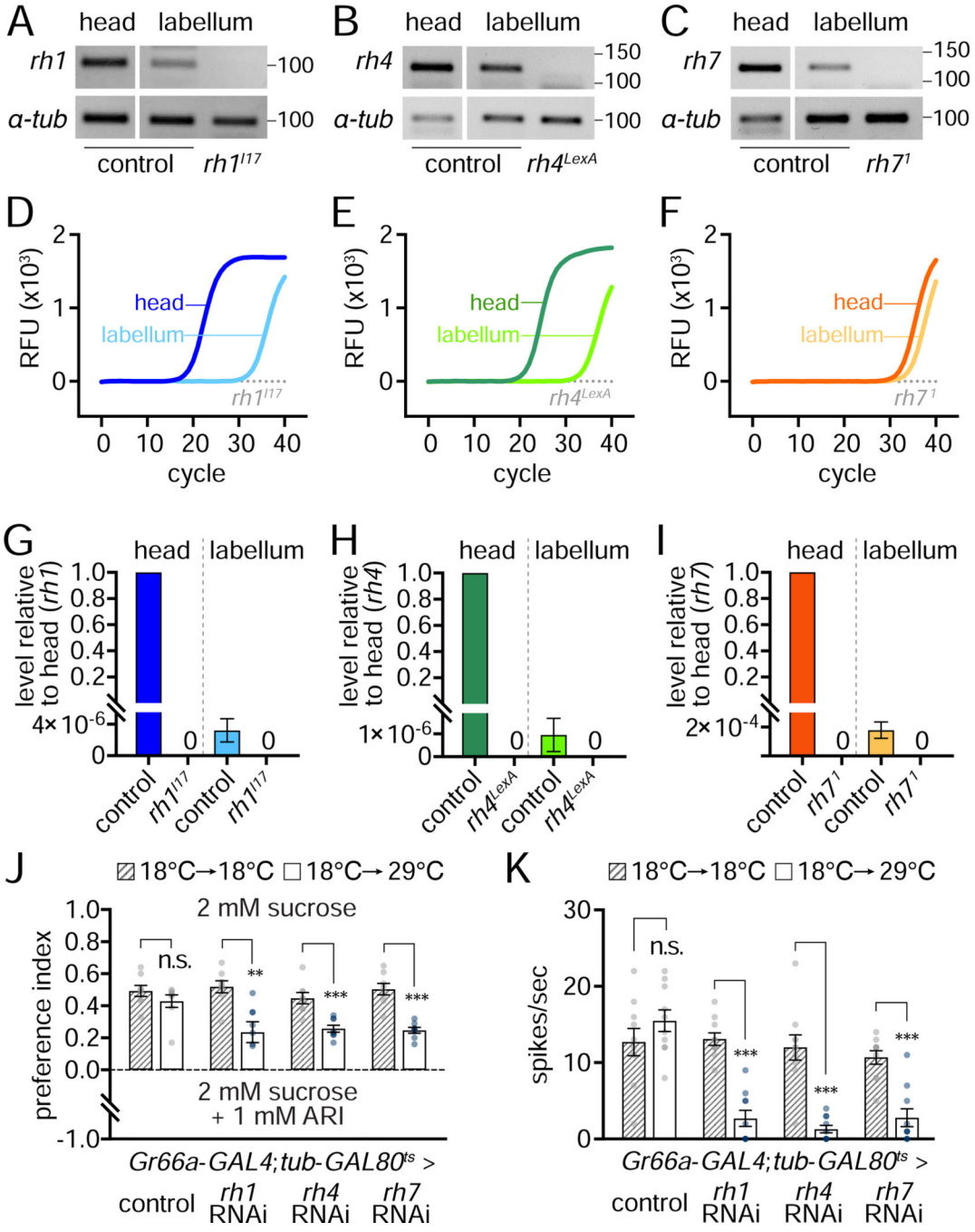

Figure 4. Expression of *opsins* in the labellum

(A–C) RT-PCR products of **(A)** *rh1*, **(B)** *rh4*, and **(C)** *rh7* using cDNA from control (w^{1118}) heads without labella, control labella, or mutant labella. *α-tubulin* (*α-tub*) served as the internal control.

(D–F) Quantitative RT-PCR amplification curves using cDNA from control heads without labella, control labella, or mutant labella. The data are the mean of 3 independent experiments. RFU, relative fluorescent units.

(G–I) *opsin* transcript levels relative to the control head obtained from quantitative RT-PCR reactions using cDNA from control heads without labella, control labella, or mutant labella. Means ±SEMs from ≥3 independent experiments. See also Figure S4M.

(D,G) *rh1* transcripts in control heads (blue), control labella (light blue), and $rh1^{I17}$ labella (gray).

(E,H) *rh4* transcripts in control heads (green) control labella (light green), and $rh4^{LexA}$ labella (gray).

(F,I) *rh7* transcripts in control heads (orange), control labella (light orange), and $rh7^{1}$ labella (gray).

(J,K) Effects of RNAi knockdown of *rh1*, *rh4*, or *rh7*, specifically in adult flies, on the responses to aristolochic acid (ARI). The *UAS-RNAi* lines were expressed using the *Gr66a-GAL4*. Temperature control of GAL4 activity was mediated by the temperature-sensitive GAL4 inhibitor, $GAL80^{ts}$ (*tub-GAL80*^{ts}). $GAL80^{ts}$ is active and inactive at 18° and 29°C, respectively. Flies were either 1) raised at 18°C and maintained at 18°C following eclosion (gray; 18°C→18°C; no RNAi), or 2) raised at 18°C and transferred to 29°C upon eclosion (white; 18°C→29°C; RNAi in adults only).

(J) Two-way choice feeding assays testing preferences for 2 mM sucrose versus 2 mM sucrose plus 1 mM ARI. n=8 per genotype. Means ±SEMs. Statistics were performed using the unpaired Student's *t*-test.

(K) Quantification of tip recording action potentials between 200–1200 msec following application of 1 mM ARI. n=8 per genotype. Means ±SEMs. Statistics were performed using the unpaired Student's *t*-test.

** $p<0.01$ and *** $p<0.001$.

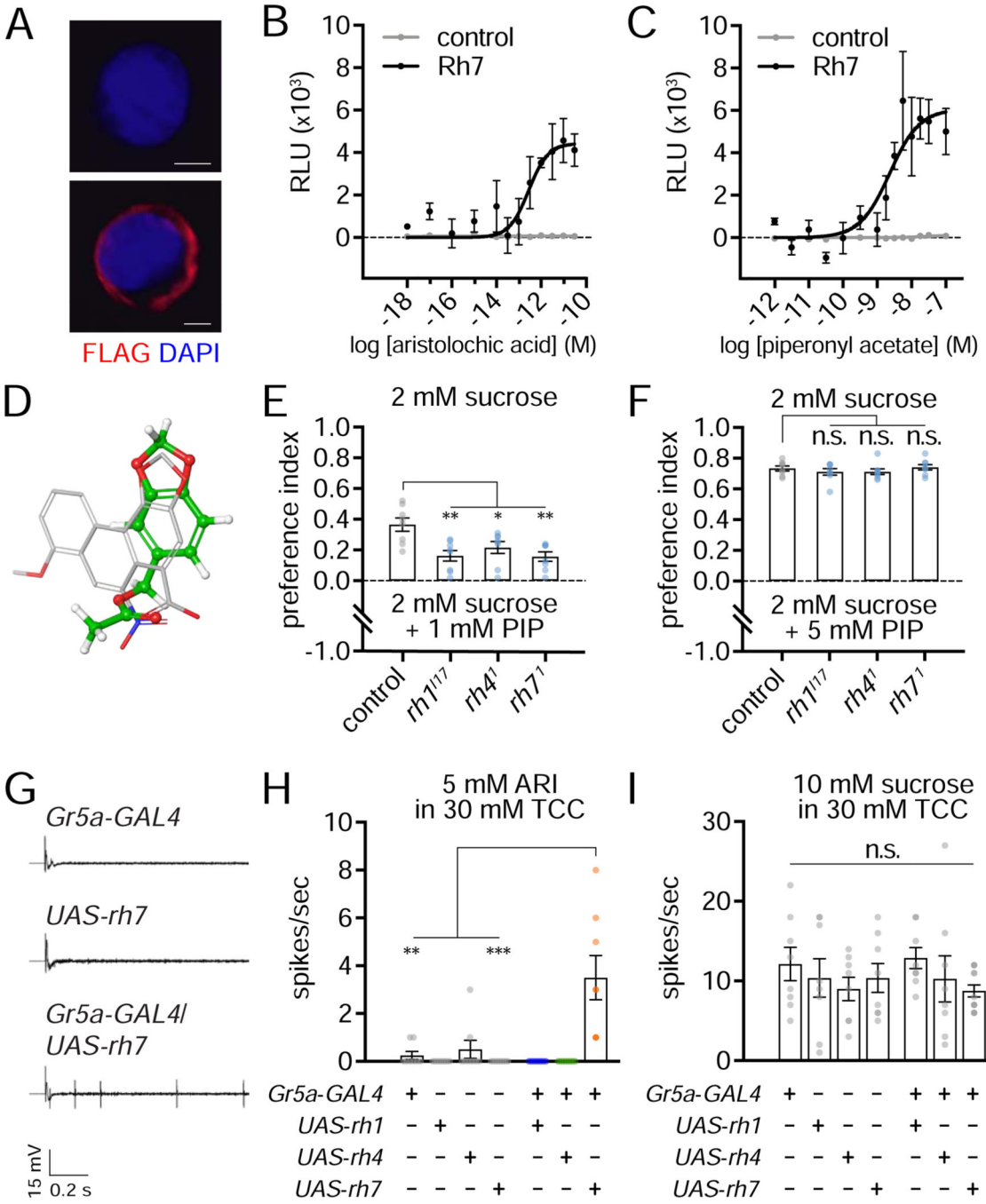

Figure 5. Activation of Rh7 *in vitro*

(A) HEK293T cells expressing the empty vector (control; top) and the vector encoding FLAG::Rh7 (bottom). Anti-FLAG (red) and DAPI nuclear stain (blue). Scale bars indicate 5 μm. See also Figures S5A and S5B.

(B,C) Normalized dose responses of control cells (gray) and FLAG::Rh7-expressing cells (black) stimulated with **(B)** aristolochic acid and **(C)** piperonyl acetate. Activities assessed using a β-arrestin recruitment assay [31]. Signals are normalized to the vehicle control baseline. n=4 per concentration. Means ±SEMs. RLU, relative luminescence units.

(D) Superimposition of the piperonyl acetate (green) and aristolochic acid structures (white). See also Figures S5C and S5D.

(E,F) Testing preferences of control, *rh1*^{I17}, *rh4*^{1}, and *rh7*^{1} flies for 2 mM sucrose versus 2 mM sucrose plus **(E)** 1 mM piperonyl acetate or **(F)** 5 mM piperonyl acetate (PIP), using two-way choice feeding assays. n=8 per genotype. Means ±SEMs. Statistics were performed using one-way ANOVA with Tukey's multiple comparisons tests.

(G) Representative tip recording traces obtained by stimulating L4 sensilla of the indicated flies with 5 mM aristolochic acid (ARI) in 30 mM TCC.

(H) Quantification of tip recording action potentials of flies ectopically expressing *rh1*, *rh4*, or *rh7* in sugar-responsive neurons (using the *Gr5a-GAL4*) between 200–1200 msec following application of 5 mM ARI in 30 mM TCC to L4 sensilla. n=8 per genotype. Means ±SEM. Statistics were performed using Kruskal-Wallis test with the Dunn's multiple comparisons test.

(I) Quantification of tip recording action potentials of flies ectopically expressing *rh1*, *rh4*, or *rh7* in sugar-responsive neurons (using the *Gr5a-GAL4*) between 200–1200 msec following application of 100 mM sucrose in 30 mM TCC to L4 sensilla. n=8 per genotype. Means ±SEMs. Statistics were performed using one-way ANOVA with a Tukey's multiple comparisons test.

* $p<0.05$, ** $p<0.01$, and *** $p<0.001$.

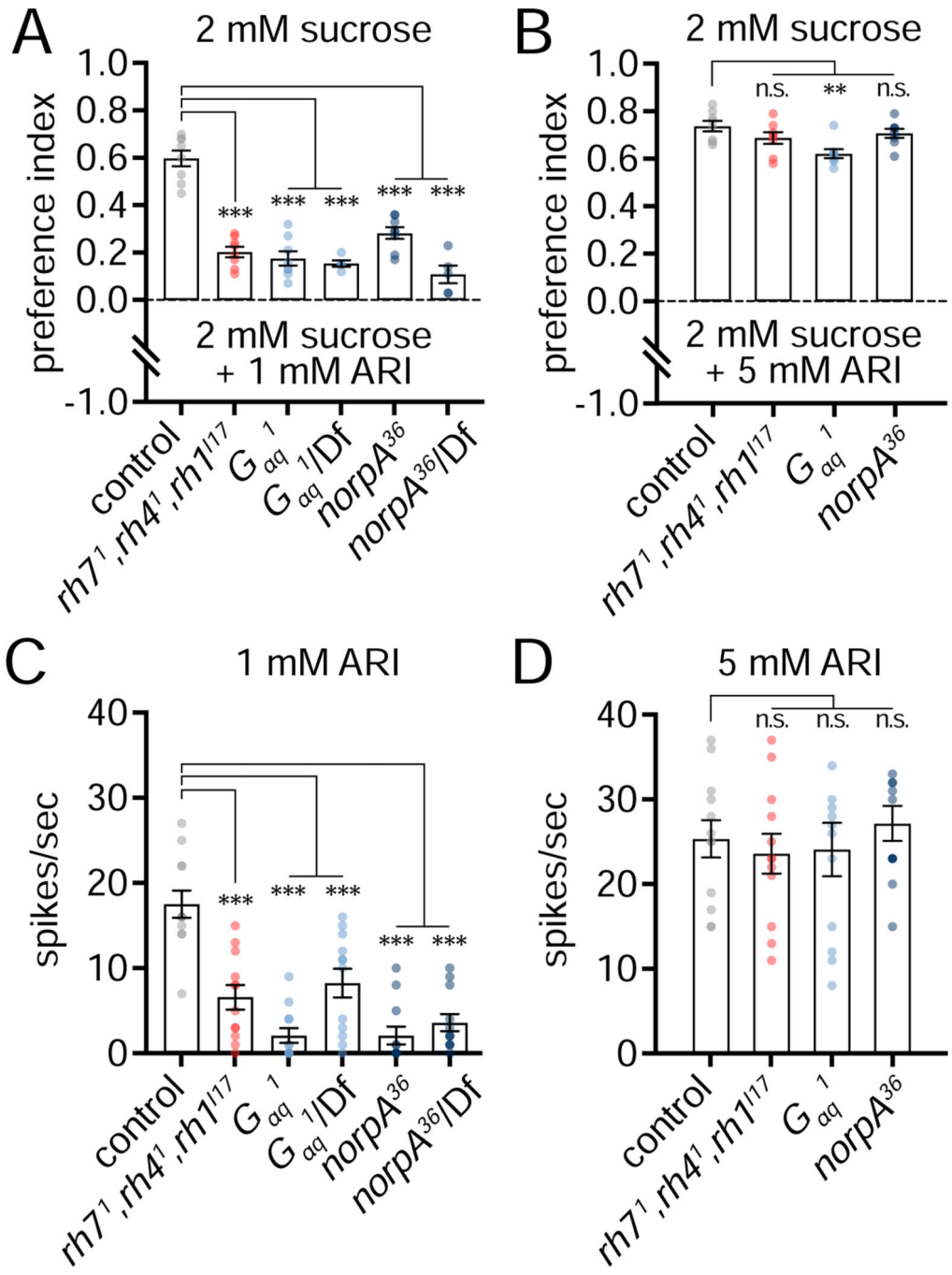

Figure 6. G_q-PLCβ signaling functions in sensation of lower concentrations of aristolochic acid

(A,B) Two-way choice feeding assays testing the preferences for 2 mM sucrose versus 2 mM sucrose plus **(A)** 1 mM aristolochic acid (ARI) or **(B)** 5 mM ARI. n=5–8 per genotype. Df indicates a deficiency line. Means ±SEMs. Statistics for the *opsin* triple mutant was performed using the unpaired Student's *t*-test. The statistics for $G_{\alpha q}$ and *norpA* alleles were performed using one-way ANOVA with Tukey's multiple comparisons test.

(C–D) Quantification of tip recording action potentials between 200–1200 msec following application of **(C)** 1 mM ARI or **(D)** 5 mM ARI. n=12 per genotype. Means ±SEMs. The

statistics for the *opsin* triple mutant was performed using the MannWhitney test. The statistics for the G_{aq} and *norpA* alleles were performed using the Kruskal-Wallis test with Dunn's multiple comparisons test. See also Figure S6.

** $p<0.01$ and *** $p<0.001$.

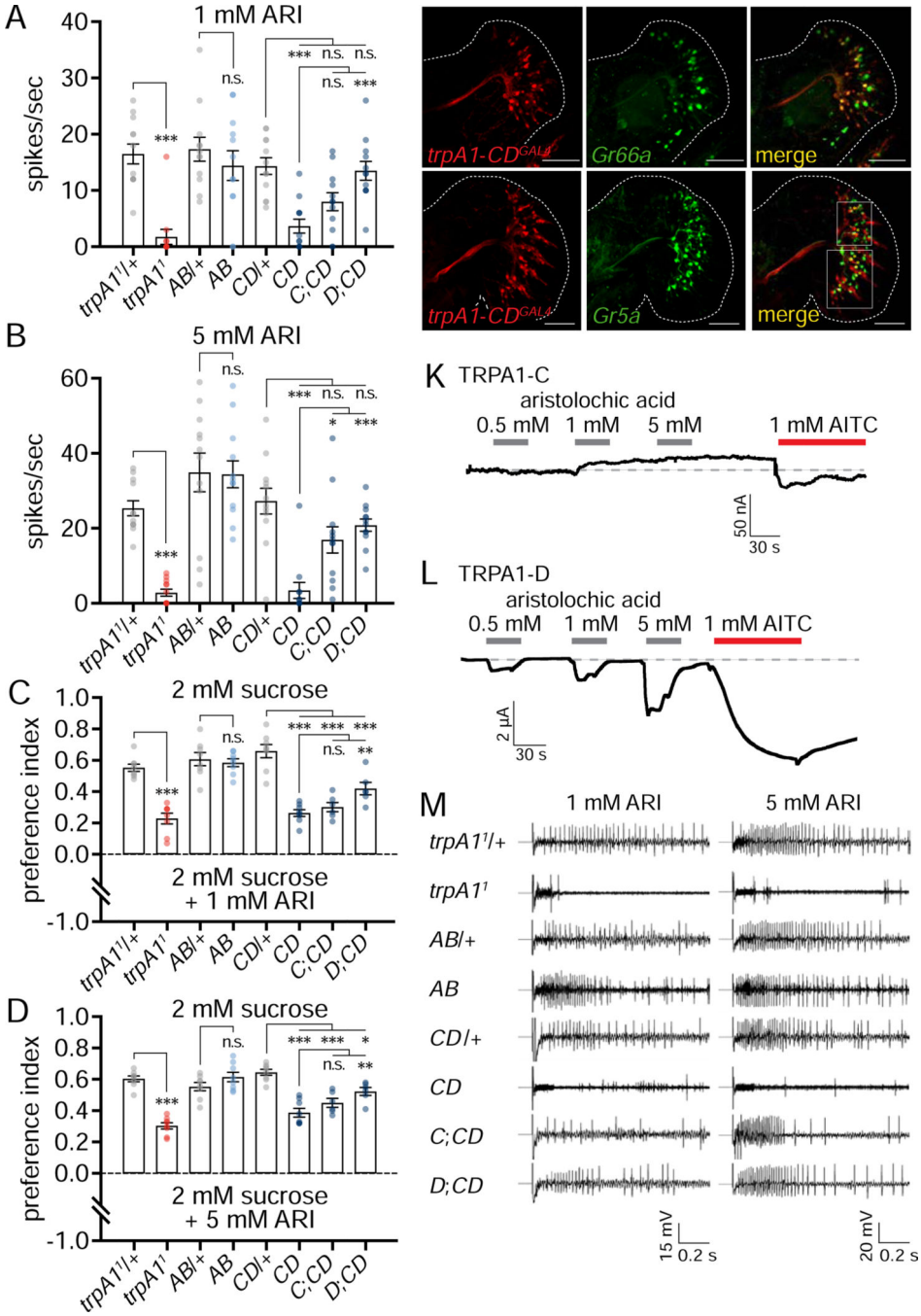

Figure 7. Role of TRPA1 isoforms in sensing aristolochic acid

Testing requirements for *trpA1* isoforms in responding to aristolochic acid: *trpA1*^{1} (null mutant), *trpA1-AB*^{GAL4} (*AB*; disrupting *A* and *B* isoforms; see also Figure S7C), *trpA1CD*^{GAL4} (*CD*; disrupting *C* and *D* isoforms; see also Figure S7C), and the *trpA1-CD*^{GAL4} mutant expressing either the *UAS-trpA1-C* (*C*;*CD*) or *UAS-trpA1-D* (*D*;*CD*) transgenes.

(A,B) Quantification of tip recording action potentials between 200–1200 msec following application of **(A)** 1 mM aristolochic acid (ARI) and **(B)** 5 mM ARI. n=12 per genotype.

Means ±SEMs. Statistics for *trpA1* and *AB* were performed using the Mann-Whitney test. Statistics for *CD* and *CD* isoform rescues were performed using the Kruskal-Wallis test with Dunn's multiple comparisons test.

(C,D) Two-way choice feeding assays testing the preferences for 2 mM sucrose alone versus 2 mM sucrose plus **(C)** 1 mM ARI and **(D)** 5 mM ARI. n=6–8 per genotype. Means ±SEMs. Statistics for *trpA1* and *AB* were performed using the unpaired Student's *t*-test. Statistics for the *CD* and *CD* isoform rescues were performed using one-way ANOVA with Tukey's multiple comparisons test.

(E–G) Confocal images of labella showing expression of **(E)** *UAS-dsRed* driven by *trpA1-CD^{GAL4}*, **(F)** *Gr66a-I-GFP*, and **(G)** merge. Tissues were stained with anti-dsRed (red) and anti-GFP (green). Scale bars indicate 50 μm.

(H–J) Confocal images of labella showing expression of **(H)** *UAS-dsRed* driven by *trpA1-CD^{GAL4}*, **(I)** *Gr5a-I-GFP*, and **(J)** merge. Tissues were stained with anti-dsRed (red) and anti-GFP (green). Scale bars indicate 50 μm. Asterisks indicate separate cell bodies that do not co-label. See Figure S7J for boxed regions.

(K–L) Two-electrode voltage clamp recordings using *Xenopus* oocytes injected with **(K)** *trpA1-C* or **(L)** *trpA1-D* cRNA. The oocytes were perfused with the indicated concentrations of ARI followed by 1 mM allyl isothiocyanate (AITC). Shown are the whole-cell inward currents.

(M) Representative tip recording traces of Figures 7A and 7B obtained by stimulating S6 sensilla with 1 mM ARI and 5 mM ARI, respectively. The genotypes are indicated.

* $p<0.05$, ** $p<0.01$, and *** $p<0.001$.